Chemical assessment of the explosive chamber in the projector system of Hayabusa2 for asteroid sampling

Yoshinori Takano (takano@jamstec.go.jp)
JAMSTEC https://orcid.org/0000-0003-1151-144X
Keita Yamada
Tokyo Institute of Technology
Chisato Okamoto (Deceased)
Kobe University
Hirotaka Sawada
ISAS/JAXA
Ryuji Okazaki
Kyushu University
Kanako Sakamoto
ISAS/JAXA
Yoko Kebukawa
Yokohama National University
Kento Kiryu
Yokohama national University
Takazo Shibuya
JAMSTEC
Motoko Igisu
JAMSTEC
Hajime Yano
ISAS/JAXA
Shogo Tachibana
Univ Tokyo

Technical report

Keywords: abiogenic organic molecules, aliphatic and aromatic hydrocarbons, explosion products, nominal and off-nominal assessment, energetic reaction with quenching effect

Posted Date: June 16th, 2020

DOI: https://doi.org/10.21203/rs.3.rs-19041/v2

Version of Record: A version of this preprint was published on July 11th, 2020. See the published version at https://doi.org/10.1186/s40623-020-01217-y.

Assessment of the explosive chamber in the projector system of Hayabusa2 for asteroid sampling

Yoshinori Takano[1], Keita Yamada[2], Chisato Okamoto[3], Hirotaka Sawada[4], Ryuji Okazaki[5], Kanako Sakamoto[6], Yoko Kebukawa[7], Kento Kiryu[8], Takazo Shibuya[9], Motoko Igisu[10], Hajime Yano[11], Shogo Tachibana[12] and Hayabusa2 project team[13]

Author #1: Yoshinori Takano*,
Japan Agency for Marine-Earth Science and Technology (JAMSTEC),
Natsushima, Yokosuka 237-0061, Japan.
https://orcid.org/0000-0003-1151-144X

Author #2: Keita Yamada,
Department of Environmental Chemistry and Engineering,
Tokyo Institute of Technology, Yokohama, 226-8503 Kanagawa, Japan.

Author #3: Chisato Okamoto (Deceased),
Department of Planetology, Kobe University,
1-1, Rokkodai-cho, Kobe 657-8501, Japan.

Author #4: Hirotaka Sawada,
Institute of Space and Astronautical Science (ISAS),
Japan Aerospace Exploration Agency (JAXA),
3-1-1 Yoshinodai, Sagamihara, Kanagawa 252-5210, Japan.

Author #5: Ryuji Okazaki,
Department of Earth and Planetary Science, Kyushu University,

744 Motooka, Nishi-ku, Fukuoka 819-0395, Japan.

Author #6: Kanako Sakamoto,
Institute of Space and Astronautical Science (ISAS),
Japan Aerospace Exploration Agency (JAXA),
3-1-1 Yoshinodai, Sagamihara, Kanagawa 252-5210, Japan.

Author #7: Yoko Kebukawa,
Graduate School of Engineering Science, Yokohama National University,
79-5 Tokiwadai, Hodogaya-ku, Yokohama 240-8501, Japan.
https://orcid.org/0000-0001-8430-3612

Author #8: Kento Kiryu,
Graduate School of Engineering Science, Yokohama National University,
79-5 Tokiwadai, Hodogaya-ku, Yokohama 240-8501, Japan

Author #9: Takazo Shibuya,
Japan Agency for Marine-Earth Science and Technology (JAMSTEC),
Natsushima, Yokosuka 237-0061, Japan.

Author #10: Motoko Igisu,
Japan Agency for Marine-Earth Science and Technology (JAMSTEC),
Natsushima, Yokosuka 237-0061, Japan.

Author #11: Hajime Yano,
Institute of Space and Astronautical Science (ISAS),
Japan Aerospace Exploration Agency (JAXA),
3-1-1 Yoshinodai, Sagamihara, Kanagawa 252-5210, Japan.

Author #12: Shogo Tachibana,
UTokyo Organization for Planetary and Space Science, University of Tokyo,
7-3-1 Hongo, Tokyo 113-0033, Japan.
&
Institute of Space and Astronautical Science (ISAS),
Japan Aerospace Exploration Agency (JAXA),
3-1-1 Yoshinodai, Sagamihara, Kanagawa 252-5210, Japan.
https://orcid.org/0000-0002-4603-9440

Author #13: Hayabusa2 project team
Institute of Space and Astronautical Science (ISAS)/
Japan Aerospace Exploration Agency (JAXA),
3-1-1 Yoshinodai, Sagamihara, Kanagawa 252-5210, Japan.

*Corresponding author, E-mail: takano@jamstec.go.jp

Abstract

We report an assessment of the explosive chamber in the projector system used during the sampling operation of the Hayabusa2 project at the surface of the C-type asteroid Ryugu. Although the explosion process was designed as a closed system (cf. Sawada et al., Space Sci. Rev., 2017), volatile combustion gases and semivolatile organics were produced together with quenched carbonaceous products. The chemical compositions of the gases, organics, and inorganics were investigated in the screening analysis. A solid-phase microextraction technique and thermal desorption coupled with gas chromatography/mass spectrometry analysis revealed that aliphatic (<C_{20} *n*-alkanes) and aromatic (<pyrene) hydrocarbons were produced in the closed chamber system. The aromatic ring compositions of the latter showed a semilogarithmic decrease: one ring > two rings > three rings > four rings, resulting in abiogenic molecular patterns. The most intense inorganic fingerprints were due to potassium (K^+) and chloride (Cl^-) ions derived from the initial KTB explosive and RK ignition charge. We discuss quality control and quality assurance issues applicable to future sample processes during the Hayabusa2 project.

Keywords

abiogenic organic molecules, aliphatic and aromatic hydrocarbons, explosion products, nominal and off-nominal assessment, energetic reaction with quenching effect

1. Introduction

Hayabusa2 is a sample-and-return mission to the C-type asteroid (162173) Ryugu to achieve a comprehensive understanding of the evolutionary history of the solar system (e.g., Tachibana et al., 2014). The Hayabusa2 spacecraft found that Ryugu is a dark rubble pile body, and hydrated silicates are ubiquitous on its surface (Watanabe et al., 2019; Kitazato et al., 2019; Sugita et al., 2019). The spacecraft successfully performed two sampling operations on the Ryugu surface materials, which will be returned to Earth in late 2020. The basic concept of the Hayabusa2 sampling system has been described previously (e.g., Tachibana et al., 2014; Sawada et al., 2017; Okazaki et al., 2017). To collect enough sample (~100 mg) from the Ryugu surface, each 5-g Ta projectile was used at the time of touch-down during the sampling operation (Sawada et al., 2017). The projectile shooting operation has three steps: (1) explosion in the explosive chamber; (2) acceleration of the projectile by the combustion gas within the closed sabot system; and (3) projectile shooting at ~300 m s^{-1} after separation from the sabot using combustion gas stored in the explosive chamber (Figure 1). To date, the chemical properties of the explosive products, including deflagration and detonation processes, have been investigated mainly in terms of the formation of solid materials, including amorphous carbon composites, shocked graphite, and occasionally diamond (e.g., Greiner et al., 1988; Titov et al., 1989; Kuznetsov et al., 1994; Chen et al., 2003; Mansurov, 2005).

Here, we note that the explosion for projectile shooting occurs in the closed system inside the projector during the nominal operation case (Sawada et al., 2017) and that the explosive products that we report in this study are not considered to be mixed with the returned sample except in the off-nominal case, where the leakage of explosive products occurs from the projector. We also note that we have previously studied the analytical pathways in Hayabusa based on an investigation of category 3 carbonaceous particles, which indicated analogous potential contaminants that could be observed throughout the sampling processes of Hayabusa2 (e.g., Ito et al., 2014; Yabuta et al., 2014; Uesugi et al., 2014; Naraoka et al., 2015; Kitajima et al., 2015).

The explosive products for projectile shooting are potential contaminants of Hayabusa2-returned Ryugu samples. However, the chemical compositions and functional groups of the volatile and nonvolatile organic compounds preserved in the soot products are largely unknown, including those of labile organic compounds. In this study, we assessed the projector system in terms of the chemical composition of the volatile gases and nonvolatile organic compounds in a laboratory-based simulation experiment, which should provide useful information on contaminants for curation and analysis of the returned samples.

2. Assessment procedure

2.1. Explosion experiments in the closed system

The Hayabusa (MUSES-C) impact sampling system (*i.e.*, "sampler") including the projector sub-system was originally designed and developed by Yano et al. (2002), Fujiwara and Yano (2005), and Yano et al. (2006). The Hayabusa2's sampling system added minor modification from the Hayabusa sampler while its projector sub-system kept its original design, which was jointly developed by ISAS, Tohoku University and Nichiyu Giken, Co, Ltd.

To simulate the explosive chamber in the projector (Tachibana et al., 2014), we performed an experiment using identical components (*i.e.*, equivalent to the flight model; Sawada et al., 2017) for the KTB explosive ($KClO_4$, 69.5%; TiH_2, 19.5%; B, 9.5%; and nitrocellulose, 1.5%) with an RK ignition charge ($Pb(SCN)_2$, ~50%; $KClO_3$, ~50%; and nitrocellulose, ≤1%; the chemical formula is shown in Figure 2) under ambient temperature and low pressure (<40 Pa, with Ar gas evacuated). Figure 3 shows the configuration of the experimental explosion chamber at the Institute of Space and Astronautical Science (ISAS), Sagamihara, Japan.

The schematic illustration (Figure 3-f) shows the projectile chamber, explosive chamber, and sample port for gas cylinders. After the explosion in the closed chamber, a gas sample was collected, together with quenched solid samples and relic materials

(Figure 4). We conducted the simulation with and without the sabot equipment for the purpose of nominal and off-nominal verification. All glassware used in the assessment was cleaned beforehand by heating at 450°C for 5 h in air to remove any artifact materials of organic contaminants.

2.2. Analysis of the volatile gas molecules by SPME-GC/MS

The volatile organic compounds (VOCs) contained in the gas sample were analyzed by gas chromatography/mass spectrometry (GC/MS). The gas sample was injected into the GC/MS system using a gastight syringe following solid-phase microextraction (SPME) (Arthur and Pawliszyn, 1990), and these techniques have been successfully applied in a wide variety of fields (e.g., Ligor et al., 2007; Wang et al., 2009; Szmigielski et al., 2012; Tuckey et al., 2013; García et al., 2014). Briefly, SPME was conducted with an 85-μm fiber coated with carboxen–polydimethylsiloxane (Carboxen^{TM}–PDMS StableFlex^{TM}; Supelco; PA, USA). The VOCs were extracted for 60 min at 60°C, after which the fiber was transferred to the injection port of the GC–MS system (Agilent 5975C GC/MSD, Agilent Technologies, Inc.), which was maintained at 240°C for 5 min, and the sample was injected in splitless mode. A capillary column (CP-PoraBOND Q, 25 m × 0.32 mm i.d.; 5 μm film thickness; Varian, CA, USA) was used for chromatographic separations. The GC oven was kept at 35°C for 5 min and then ramped up at 15°C min^{-1} to 120°C for 10 min before ramping at 50°C min^{-1} to 200°C for 6 min. The helium carrier gas flow rate was 1.5 mL min^{-1} in constant flow mode. The quadrupole MS system was operated in electron ionization mode with a scan range of m/z = 10–500. To avoid memory effects, the SPME fiber was conditioned at 250°C for 10 min before each measurement. Compounds were identified by comparison with data in the mass spectral library (Wiley Registry of Mass Spectral Data, 7th edition) included with MSD ChemStation software (Agilent Technologies, Inc.).

2.3. Analysis of the semivolatile molecules by TD-GC/MS

The semivolatile compounds were analyzed by on-line thermal desorption (TD)-GC/MS using a multipurpose sampling and thermal desorption system (MSTD-258M; GL Science Inc.) and a purge and trap device (P&T; Gestel TDS A2, Gestel Inc.) coupled to a GC/MS system (Agilent 6890N and 5973 MSD; Agilent Technologies Inc.). The MSTD sampling chamber was a quartz vessel 90 mm in diameter and 40 mm in height. The thermal desorption program was as follows. The chamber was purged with N_2 at 340 mL min^{-1} for 1 min at 280°C. The trapping time was 30 min with an N_2 flow rate of 150 mL min^{-1}. The out-gas cold trap was maintained at temperatures below –100°C in the TDS unit. A DB-5MS capillary column (30 m x 0.25 mm i.d.; 0.52 μm film thickness; Agilent Technologies Inc.) was used for chromatographic separations, and MS compound detection was achieved in electron impact mode. The GC oven temperature was programmed as follows: initial temperature of 40°C for 3 min; ramped up at 9°C min^{-1} to 220°C, then at 10°C min^{-1} to 280°C where it was maintained for 5 min. The He carrier gas flow rate was 1.5 mL min^{-1}.

2.4. Analysis of the inorganic ions and elements in solid soot

The analyses of inorganic water-soluble cations and anions involved ion chromatography (IC; DX-120 for cations; DX-500 for anions; Dionex Inc.) with Ion Pac CS10 and Ion Pac AS17 columns for cations and anions, respectively (Dionex Inc.). Gradient elution was conducted with three solvents: 25 mM methanesulfonic acid, 1.2 M methanol, and 0.95 M acetonitrile at a flow rate of 1.0 mL min^{-1} for cations and H_2O, 5 mM NaOH, and 100 mM NaOH at a flow rate of 1.5 mL min^{-1} for anions. For metal elemental analyses, inductively coupled plasma-mass spectrometry (ICP-MS; 7500s, Agilent Technologies. Inc) was used for environmental assessment. For further profiling of the solid products, we also performed qualitative micro-X-ray fluorescence analysis (μXRF) of the carbonaceous soot using an XGT-5000S system (Horiba Ltd.) with a resolution of 10 μm for surface imaging.

2.5. Fourier transform infrared spectroscopy

As a nondestructive spectroscopic technique, we performed Fourier transform infrared (FT-IR) spectroscopy following the procedure described in Kebukawa et al. (2020). Infrared absorption spectra were collected from a small amount of sample pressed onto a KBr plate (~5 × 5 × 1 mm^3) using a micro-FT-IR instrument (JASCO FT/IR-6100+IRT-5200) equipped with a ceramic IR light source, a germanium-coated KBr beam splitter, a mercury-cadmium-telluride (MCT) detector, and ×16 Cassegrainian mirrors. A total of 128 scans of the IR transmission were accumulated with a wavenumber resolution of 8 cm^{-1} in the wavenumber range of 4000-700 cm^{-1} and with a 50 × 50 μm^2 aperture for each spectrum. Background spectra were acquired from the blank areas of the KBr plate adjacent to the samples.

2.6. Raman spectroscopy

A sample was directly analyzed by an established method (after Kiryu et al., 2019) using a Raman spectrometer (Nanophoton RAMAN touch). In brief, a 532 nm laser was used, and the laser beam was focused through a ×20 objective. The spot size was ~1 μm (×20 objective with a numerical aperture of 0.45), and the laser power at the sample surface was ~700 μW. The spectral range was 100–2600 cm^{-1}, and a grating of 600 grooves mm^{-1} was used. The exposure time for each spectrum was 20 s, and two accumulations were obtained for each analytical spot to correct for cosmic rays. The Raman shift was calibrated using a silicon wafer prior to the analytical procedure.

3. Results and discussion

3.1. Volatile and semivolatile molecules from the explosion

The VOCs detected in the projectile chamber included CH_4 (19.8 μmol carbon (μmol C) L^{-1}), C_2H_4 (0.9 μmol C L^{-1}), C_2H_6 (0.6 μmol C L^{-1}), and benzene (0.4 μmol C L^{-1}) (Figure 5). The methane/ethane ratio (C_1/C_2) was 33.0, which is unlike the value of 1.04 found for the Murchison meteorite (methane, 8.9 nmol g^{-1}; ethane, 8.5 nmol g^{-1}; data

from Yuen et al., 1984). The low-molecular-weight carboxylic acids (including acetic acid) and various other organic molecules detected by total ion chromatogram (TIC) on the TD-GC/MS are shown in Figure 6a. A wide range of aliphatic hydrocarbons, including straight chain alkanes (<*n*-$C_{20}H_{42}$), were detected in the extracted ion chromatogram (EIC, *m/z* = 57).

A number of polycyclic aromatic hydrocarbons (PAHs) and heterocyclic hydrocarbons were identified (Figure 6b–d), with the most abundant being benzene (*m/z* = 78) and toluene (*m/z* = 91 and 92 with benzyl cation isomerism; Appendix), which is consistent with the results of volatile gas analysis by GC/MS. C_2-Alkylbenzenes (*m/z* = 106), including ethyl benzene and xylene (*o*-, *m*-, and *p*-), were also observed. Naphthalene (*m/z* = 128) was the most abundant bicyclic species among the isomers of methyl- and dimethyl-naphthalene (*m/z* = 142 and 156, respectively). The experimentally derived ratios of methyl naphthalene isomers (2-methyl (β-configured) to 1-methyl (α-configured) naphthalene) (Radke et al., 1982) obtained with and without the sabot device were 1.50 and 1.27, respectively, which are similar to the ranges reported for carbonaceous meteorites (Yamato-790112, ~2.02; Murchison, ~1.86; Renazzo, ~1.44; Pearson et al., 2006) and products of impact shock experiments of benzene (Mimura, 1995). Biphenyl (*m/z* = 154), acenaphthene (*m/z* = 154), fluorene (*m/z* = 166), and phenanthrene/anthracene (*m/z* = 178) are also known as abiogenic bicyclic and tricyclic aromatics. The detection of tri- and tetracyclic aromatics and heterocyclic methyl phenanthrene (*m/z* = 192), fluoranthene/pyrene (*m/z* = 202), and dibenzofuran (*m/z* = 168) indicates that aromatic cyclization processes occurred in the explosion and quenching processes. The relative abundance of the aromatic compounds and their isomers decreases semilogarithmically with increasing chain length, *i.e.*, 1 ring (benzene) > 2 rings (naphthalene) > 3 rings (phenanthrene) > 4 rings (pyrene), in experiments both with and without the sabot device (Figure 7). The semilogarithmic linear relations between PAHs (X*n*: number of rings) and their relative abundance % (Y; benzene as 100) are expressed as,

$$\ln Y = -1.78\ Xn + 6.15\ (R^2 = 0.99);\ \text{with sabot} \quad [1]$$

$$\ln Y = -1.49\ Xn + 5.60\ (R^2 = 0.99);\ \text{without sabot} \quad [2]$$

Therefore, these linear relations imply a stepwise cyclization in which larger PAHs are formed from their smaller homologues (e.g., following the pathways for the pyrene series and the fluoranthene series proposed by Naraoka et al., 2000).

3.2. Inorganic ions and elements extracted from solid soot

The most abundant inorganic ions from the water-extractable fractions were Cl^- and K^+ derived from the KTB explosive and RK ignition charge components (Supplementary Figure 1). The other significant inorganic ions were shown to be nitrates (NO_2^-, NO_3^-), halogens (Br^-, F^-), organic acids (acetic acid, formic acid), sulfate (SO_4^{2-}), phosphate (PO_4^{3-}) and ammonium (NH_4^+) by ion chromatography (IC). Sodium (Na), aluminum (Al), magnesium (Mg), titanium (Ti) and other elements were also observed in the solid soot by ICP-MS. Figure 8 presents the surface imaging analysis of the solid soot products observed by μXRF, implying heterogeneous precipitation of solid products after the reaction of the KTB and RK explosives and the subsequent quenching effect.

3.3. IR and Raman spectra

The IR spectra were obtained at >10 different positions on the soot sample. Figure 9 shows representative IR spectra from several spots in the region of interest. Although the peak positions are mostly common, the peak intensity ratios vary substantially. Three peaks are commonly observed at ~1640, ~1515, and ~1415 cm^{-1}. There are fine peaks at 1100, 1000, 940, and 860 cm^{-1}. The possible peak assignments based on Socrates (2004) are shown in Table 1. The spectra from some spots show a peak at 3417 cm^{-1} due to N-H, in addition to a broad O-H band at ~3400 cm^{-1}, which is mostly due to adsorbed water, indicating that the sample is hydrophilic.

Mapping analysis in a 1350 μm × 400 μm region shows heterogeneity at the ~100

μm scale—there are two groups of IR absorptions (Figure 10). One is distributed mainly in the right area and includes bands at 860, 1000, 1100, and 1830 cm^{-1}. The other is distributed in three regions: left, middle, and right, and includes the bands at 940, 1410, 1520, and 1640 cm^{-1}. The black and white materials are indicated by the optical microscopic image (Figure 9-b). The black materials show less intense IR signals compared to the white materials (Figures 9-a and 10).

The Raman spectra obtained from the soot sample are characterized by an intense peak at 1095 cm^{-1} with weaker peaks mostly below ~750 cm^{-1} (Figure 11, Table 1). The Raman features from the black materials are mostly common with those of the white materials—although some peaks were slightly shifted and weaker than the corresponding peaks from the white materials. Considering that the IR features from the black materials are also weaker than those of white materials, the black materials could be IR and Raman inactive. Assuming the IR and Raman characteristics, the soot sample (the white materials) likely contains nitrates, ammonium/amine salts, carbonates, and sulfur oxyanions. Aromatic compounds, amides and halides might also be present. Notably, these characteristics are not definitive, and further analyses are required to identify these compounds.

Typical organic matter in chondritic meteorites shows aliphatic C-H peaks and a C=O peak at around 2900 cm^{-1} and ~1700 cm^{-1}, respectively, in the IR spectra (e.g., Kebukawa et al., 2011; Orthous-Daunay et al., 2013), and D and G bands at around 1350 cm^{-1} and 1580 cm^{-1}, respectively, in the Raman spectra (e.g., Busemann et al., 2007). These features are not observed in the soot sample.

4. Summary and perspectives

An energetic reaction involving a physicochemical explosive shock will vigorously activate of chemical substances, resulting in the abiotic synthesis of various gases and solid materials after the eventual quenching process. The KTB- and RK-based explosives produce carbonaceous debris containing various labile and refractory organic materials

that do not undergo thermal degradation, and the retrieved sample quality is guaranteed by the closed explosion system (Sawada et al., 2017).

Quality control for the sample process, including in ground-based procedures, is an important issue for sample return missions. The ESCuC (the Extraterrestrial Sample Curation Center) in the ISAS/JAXA facility (Yada et al., 2014; Uesugi et al., 2019) was assessed by an interlaboratory evaluation, and Sugahara et al. (2018) reported an assessment of the clean room at ISAS/JAXA, which is intended to be used in the processing Hayabusa2 samples (cf. assessment on the OSIRIS-REx mission; Dworkin et al., 2017). Along with those quality controls above, the analytical flow of pristine samples (*e.g.*, element profiles, chemical composition, mineralogy, isotopic signatures, organic molecules, and physical properties) definitely requires a seamless process to obtain precise and native information for the asteroid Ryugu.

Appendix.

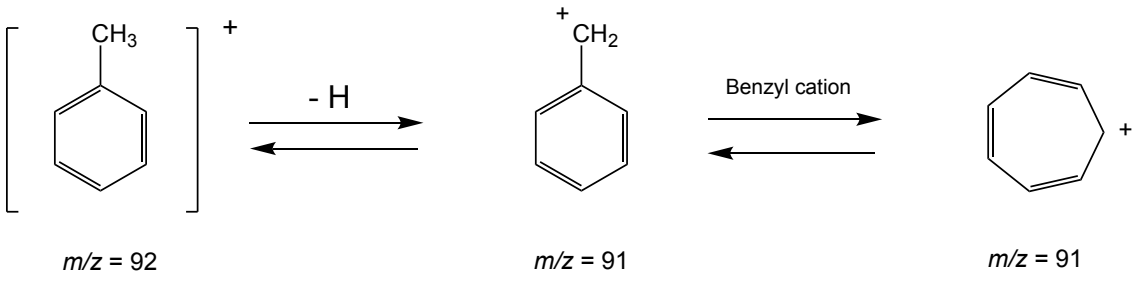

Toluene to benzyl cation isomerism *via* $m/z = 91$ and $m/z = 92$.

List of abbreviations

C-type: Carbonaceous-type, VOCs: Volatile organic compounds, PAH: polycyclic aromatic hydrocarbons, GC: gas chromatography, SPME: Solid-phase micro extraction, TDS: Thermal desorption system, GC/MS: GC coupled with mass spectrometry, TIC: total ion chromatogram, EIC: Extracted ion chromatogram, ICP-MS: Inductively coupled plasma-mass spectrometry, μXRF: micro X-ray fluorescence, FT-IR: Fourier transform infrared, ESCuC: the Extraterrestrial Sample Curation Center, OSIRIS-REx: Origins, Spectral Interpretation, Resource Identification, Security, Regolith Explorer.

Competing interests

The authors declare that they have no competing interests regarding this document.

Availability of data and materials

The movie of a shooting verification using an identical bullet, *i.e.*, equivalent products manufactured at the same time as the flight model, is provided in the website.

http://www.hayabusa2.jaxa.jp/en/topics/20190214e_Experiment/

Please contact the authors for other data requests.

Authors' contributions

YT conducted the experiments, interpreted the data, and finalized the manuscript. KY conducted the experiments for volatile gas analyses and interpreted the data. CO, KS and RO conducted the experiments and participated in upgrading the projector sub-system and in the analytical assessments. KK, YK, MI and TS performed nondestructive analyses by FT-IR and Raman spectroscopy. HY developed the Hayabusa projector sub-system while HS and ST led the upgrading activity of the Hayabusa2 projector system, according to the assessment results with YT, RO, CO, and KS. All authors contributed to the manuscript and approved the final version of the content.

Author information

The current address of KS is the Department of Earth and Planetary Science, University of Tokyo, 7-3-1 Hongo, Tokyo 113-0033, Japan.

Acknowledgments

The experiments with explosives were permitted by the Institute of Space and Astronautical Science (ISAS). We thank Akira Fujiwara, Sunao Hasegawa and Masanao Abe of ISAS/JAXA, Kazuyoshi Takayama and Koichi Okano of Tohoku University for contributing the original design and development of the Hayabusa projector sub-system. The Hayabusa2 project team is acknowledged for supervising assessment experiments of the Hayabusa2 projector. We appreciate the Space Plasma Laboratories at ISAS, JAXA, for their support in the development of the Hayabusa2 sampler as a collaborative research program. We also thank Renesas Semiconductor Manufacturing Co. Ltd. and Toshiba Nanoanalysis Corporation for their help with the assessments. Preliminary reports based on this paper were presented at Hayabusa 2015 (3rd symposium of Solar System Materials) and the Solar System Symposium in Sapporo, 2020.

Funding

This work was supported by a Grant-in-Aid for Scientific Research on Innovative Areas (Research Project on Evolution of Molecules in Space; YT, No. 25108006) by project leader Prof. Akira Kouchi (Hokkaido Univ.) from the Japan Society for the Promotion of Science (JSPS) and in part by a JSPS grant (No. 19H00712, ST; No. 16H04083, YT; No. JP17H06458, YK&TS).

References

Arthur, C.L. and Pawliszyn, J. (1990) Solid phase microextraction with thermal desorption using fused silica optical fibers. Analytical Chemistry, 62, 2145–2148. doi: 10.1021/ac00218a019.

Busemann, H., Alexander, C. M. O. D. and Nittler, L. R. (2007) Characterization of insoluble organic matter in primitive meteorites by microRaman spectroscopy. Meteoritics & Planetary Science, 42, 1387-1416. doi: 10.1111/j.1945-5100.2007.tb00581.x.

Chen, P., Huang, F. and Yun, S. (2003) Characterization of the condensed carbon in detonation soot. Carbon, 41, 2093-2099. doi: 10.1016/S0008-6223(03)00229-X

Dworkin, J.P., Adelman, L.A., Ajluni, T., Andronikov, A.V., Aponte, J.C., Bartels, A.E., Beshore, E., Bierhaus, E.B., Brucato, J.R., Bryan, B.H., Burton, A.S., Callahan, M.P., Castro-Wallace, S.L., Clark, B.C., Clemett, S.J., Connolly, H.C., Cutlip, W.E., Daly, S.M., Elliott, V.E., Elsila, J.E., Enos, H.L., Everett, D.F., Franchi, I.A., Glavin, D.P., Graham, H.V., Hendershot, J.E., Harris, J.W., Hill, S.L., Hildebrand, A.R., Jayne, G.O., Jenkens, R.W., Johnson, K.S., Kirsch, J.S., Lauretta, D.S., Lewis, A.S., Loiacono, J.J., Lorentson, C.C., Marshall, J.R., Martin, M.G., Matthias, L.L., McLain, H.L., Messenger, S.R., Mink, R.G., Moore, J.L., Nakamura-Messenger, K., Nuth, J.A., Owens, C.V., Parish, C.L., Perkins, B.D., Pryzby, M.S., Reigle, C.A., Righter, K., Rizk, B., Russell, J.F., Sandford, S.A., Schepis, J.P., Songer, J., Sovinski, M.F., Stahl, S.E., Thomas-Keprta, K., Vellinga, J.M. and Walker, M.S. (2017) OSIRIS-REx Contamination control strategy and implementation. Space Science Reviews, 214, 19. doi: 10.1007/s11214-017-0439-4.

Fujiwara, A. and Yano, H. (2005) The asteroidal surface sampling system onboard the Hayabusa spacecraft. Aeronautical and Space Sciences Japan, 53, 264-271. doi: 10.14822/kjsass.53.620_264.

García, R.A., Morales, V., Martín, S., Vilches, E. and Toledano, A. (2014) Volatile organic compounds analysis in breath air in healthy volunteers and patients

suffering epidermoid laryngeal carcinomas. Chromatographia, 77, 501–509. doi: 10.1007/s10337-013-2611-7.

Greiner, N.R., Phillips, D., Johnson, J. and Volk, F. (1988) Diamonds in detonation soot. Nature, 333, 440-442. doi: 10.1038/333440a0.

Ito, M., Uesugi, M., Naraoka, H., Yabuta, H., Kitajima, F., Mita, H., Takano, Y., Karouji, Y., Yada, T. and Ishibashi, Y. (2014) H, C, and N isotopic compositions of Hayabusa category 3 organic samples. Earth, Planets and Space, 66: 91. doi:10.1186/1880-5981-66-91.

Kebukawa, Y., Alexander, C. M. O. D. and Cody, G. D. (2011) Compositional diversity in insoluble organic matter in type 1, 2 and 3 chondrites as detected by infrared spectroscopy. Geochimica et Cosmochimica Acta. 75, 3530-3541. doi:10.1016/j.gca.2011.03.037.

Kebukawa, Y., Zolensky, M.E., Ito, M., Ogawa, N.O., Takano, Y., Ohkouchi, N., Nakato, A., Suga, H., Takeichi, Y., Takahashi, Y. and Kobayashi, K. (2020) Primordial organic matter in the xenolithic clast in the Zag H chondrite: Possible relation to D/P asteroids. Geochimica et Cosmochimica Acta, 271, 61-77. doi:10.1016/j.gca.2019.12.012.

Kiryu, K., Kebukawa, Y., Igisu, M., Shibuya, T. and Kobayashi, K. (2019) Kinetic Estimation of the Thermal Hisrory of Organic Matter in Chondrites Using Raman Spectroscopy, 82nd Annual Meeting of The Meteoritical Society. Abstract#6250.

Kitajima, F., Uesugi, M., Karouji, Y., Ishibashi, Y., Yada, T., Naraoka, H., Abe, M., Fujimura, A., Ito, M., Yabuta, H., Mita, H., Takano, Y. and Okada, T. (2015) A micro-Raman and infrared study of the several Hayabusa category 3 (organic) particles. Earth, Planets and Space, 67:20. doi:10.1186/s40623-015-0182-6.

Kitazato, K., Milliken, R., Iwata, T., Abe, M., Ohtake, M., Matsuura, S., Arai, T., Nakauchi, Y., Nakamura, T. and Matsuoka, M. (2019) The surface composition of asteroid 162173 Ryugu from Hayabusa2 near-infrared spectroscopy. Science, 364, 272-275. doi: 10.1126/science.aav7432.

Kuznetsov, V.L., Chuvilin, A.L., Butenko, Y.V., Mal'kov, I.Y. and Titov, V, M. (1994) Onion-like carbon from ultra-disperse diamond. Chemical Physics Letters, 222, 343-348. doi: 10.1016/0009-2614(94)87072-1.

Ligor, T., Szeliga, J., Jackowski, M. and Buszewski, B. (2007) Preliminary study of volatile organic compounds from breath and stomach tissue by means of solid phase microextraction and gas chromatography/mass spectrometry. Journal Breath Research, 1, 016001. doi:10.1088/1752-7155/1/1/016001.

Mansurov, Z. (2005) Soot formation in combustion processes (review). Combustion, Explosion and Shock Waves, 41, 727-744. doi: 10.1007/s10573-005-0083-2.

Mimura, K. (1995) Synthesis of polycyclic aromatic hydrocarbons from benzene by impact shock: its reaction mechanism and cosmochemical significance. Geochimica et Cosmochimica Acta, 59, 579-591. doi: 10.1016/0016-7037(95)00326-U.

Naraoka, H., Shimoyama, A. and Harada, K. (2000) Isotopic evidence from an Antarctic carbonaceous chondrite for two reaction pathways of extraterrestrial PAH formation. Earth and Planetary Science Letters, 184, 1-7. doi: 10.1016/S0012-821X(00)00316-2.

Naraoka, H., Aoki, D., Fukushima, K., Uesugi, M., Ito, M., Kitajima, F., Mita, H., Yabuta, H., Takano, Y., Yada, T., Ishibashi, Y., Karouji, Y., Okada, T. and Abe, M. (2015) ToF-SIMS analysis of carbonaceous particles in the sample catcher of the Hayabusa spacecraft. Earth, Planets and Space, 67:67. doi:10.1186/s40623-015-0224-0.

Okazaki, R., Sawada, H., Yamanouchi, S., Tachibana, S., Miura, Y., Sakamoto, K., Takano, Y., Abe, M., Itoh, S., Yamada, K., Yabuta, H., Okamoto, C., Yano, H., Noguchi, T., Nakamura, T. and Nagao, K. (2017) Hayabusa2 sample container: Metal-seal system for vacuum encapsulation of returned samples. Space Science Reviews, 208, 107-124. doi:10.1007/s11214-016-0289-5.

Orthous-Daunay, F.-R., Quirico, E., Beck, P., Brissaud, O., Dartois, E., Pino, T. and Schmitt, B. (2013) Mid-infrared study of the molecular structure variability of

insoluble organic matter from primitive chondrites. Icarus, 223, 534-543. doi: 10.1016/j.icarus.2013.01.003.

Pearson, V.K., Sephton, M. and Gilmour, I. (2006) Molecular and isotopic indicators of alteration in CR chondrites. Meteoritics & Planetary Science, 41, 1291-1303. doi: 10.1111/j.1945-5100.2006.tb00522.x

Radke, M., Willsch, H., Leythaeuser, D. and Teichmüller, M. (1982) Aromatic components of coal: relation of distribution pattern to rank. Geochimica et Cosmochimica Acta, 46, 1831-1848. doi: 10.1016/0016-7037(82)90122-3.

Sawada, H., Okazaki, R., Tachibana, S., Sakamoto, K., Takano, Y., Okamoto, C., Yano, H., Miura, Y., Abe, M., Hasegawa, S., Noguchi, T. and Hayabusa2 sampler team (2017) Hayabusa2 Sampler: Collection of asteroidal surface material. Space Science Reviews, 208, 81-106. doi: 10.1007/s11214-017-0338-8.

Socrates, G. (2004) Infrared and Raman characteristic group frequencies: tables and charts. John Wiley & Sons.

Sugahara, H., Takano, Y., Karouji, Y., Yada, T., Ohkouchi, N., Abe, M. and Hayabusa2 Project Team (2018) Amino acids on witness coupons collected from the ISAS/JAXA curation facility for the assessment and quality control of the Hayabusa2 sampling procedures. Earth, Planets and Space, 70: 194. doi: 10.1186/s40623-018-0965-7.

Sugita, S., Honda, R., Morota, T., Kameda, S., Sawada, H., Tatsumi, E., Yamada, M., Honda, C., Yokota, Y. and Kouyama, T. (2019) The geomorphology, color, and thermal properties of Ryugu: Implications for parent-body processes. Science, 364, eaaw0422. doi:0410.1126/science.aaw0422.

Szmigielski, R., Cieslak, M., Rudziński, K. J. and Maciejewska, B. (2012) Identification of volatiles from Pinus silvestris attractive for Monochamus galloprovincialis using a SPME-GC/MS platform. Environmental Science and Pollution Research, 19, 2860–2869. doi: 10.1007/s11356-012-0792-5.

Tachibana, S., Abe, M., Arakawa, M., Fujimoto, M., Iijima, Y., Ishiguro, M., Kitazato,

K., Kobayashi, N., Namiki, N., Okada, T., Okazaki, R., Sawada, H., Sugita, S., Takano, Y., Tanaka, S., Watanabe, S., Yoshikawa, M., Kuninaka, H. and Hayabusa2 project team (2014) Hayabusa2: Scientific importance of samples returned from near-Earth C-type asteroid 1999 JU3. Geochemical Journal, 48, 571-587. doi:10.2343/geochemj.2.0350.

Titov, V., Anisichkin, V. and Mal'kov, I. Y. (1989) Synthesis of ultrafine diamonds in detonation waves. Papers 9th Symposium (International) on Explosion, pp. 175-183.

Tuckey, N. P. L., Day, J. R. and Miller, M. R. (2013) Determination of volatile compounds in New Zealand Greenshell™ mussels (Perna canaliculus) during chilled storage using solid phase microextraction gas chromatography–mass spectrometry. Food Chemistry, 136, 218-223. doi: 10.1016/j.foodchem.2012.07.118.

Uesugi, M., Naraoka, H., Ito, M., Yabuta, H., Kitajima, F., Takano, Y., Mita, H., Ohnishi, I., Kebukawa, Y., Yada, T., Karouji, Y., Ishibashi, Y., Okada, T. and Abe, M. (2014) Sequential analysis of carbonaceous materials in Hayabusa-returned samples for the determination of their origin. Earth, Planets and Space, 66:102. doi:10.1186/1880-5981-66-102.

Uesugi, M., Ito, M., Yabuta, H., Naraoka, H., Kitajima, F., Takano, Y., Mita, H., Kebukawa, Y., Nakato, A. and Karouji, Y. (2019) Further characterization of carbonaceous materials in Hayabusa-returned samples to understand their origin. Meteoritics & Planetary Science, 54, 638-666. doi:10.1111/maps.13236.

Yabuta, H., Uesugi, M., Naraoka, H., Ito, M., Kilcoyne, A.L.D., Sandford, S.A., Kitajima, F., Mita, H., Takano, Y., Yada, T., Karouji, Y., Ishibashi, Y., Okada, T. and Abe, M. (2014) Molecular compositions of Hayabusa Category 3 carbonaceous particles. Earth, Planets and Space, 66:156, doi:10.1186/s40623-014-0156-0.

Yada, T., Fujimura, A., Abe, M., Nakamura, T., Noguchi, T., Okazaki, R., Nagao, K., Ishibashi, Y., Shirai, K. and Zolensky, M.E. (2014) Hayabusa‐returned sample

curation in the planetary material sample curation facility of JAXA. Meteoritics & Planetary Science, 49, 135-153. doi: 10.1111/maps.12027.

Yano, H., Hasegawa, S., Abe, M. and Fujiwara, A. (2002) Asteroidal surface sampling by the MUSES-C spacecraft. Proceedings of Asteroids, Comets, Meteors (ACM2002), ESA-SP-500, 103-106.

Yano, H., Kubota, T., Miyamoto, H., Okada, T., Scheeres, D., Takagi, Y., Yoshida, K., Abe, M., Abe, S., Barnouin-Jha, O., Fujiwara, A., Hasegawa, S., Hashimoto, T., Ishiguro, M., Kato, M., Kawaguchi, J., Mukai, T., Saito, J., Sasaki, S., and Yoshikawa, M. (2006) Touchdown of the Hayabusa spacecraft at the Muses Sea on Itokawa. Science, 312, 1350-1353. doi: 10.1126/science.1126164.

Yuen, G., Blair, N., Desmarais, D. J. and Chang, S. (1984) Carbon isotope composition of low-molecular weight hydrocarbons and monocarboxylic acids from Murchison meteorite. Nature, 307, 252-254. doi: 10.1038/307252a0.

Wang, V.-S. and Lu, M.-Y. (2009) Application of solid-phase micro extraction and gas chromatography/mass spectrometry for measuring chemicals in saliva of synthetic leather workers. Journal of Chromatography B, 877, 24–32. doi: 10.1016/j.jchromb.2008.11.006.

Watanabe, S., Hirabayashi, M., Hirata, N., Noguchi, R., Shimaki, Y., Ikeda, H., Tatsumi, E., Yoshikawa, M., Kikuchi, S. and Yabuta, H. (2019) Hayabusa2 arrives at the carbonaceous asteroid 162173 Ryugu—A spinning top–shaped rubble pile. Science, 364, 268-272. doi: 10.1126/science.aav8032.

Figure and Table legends:

Figure 1. (a) Photograph of the Hayabusa2 sampler horn (Tachibana et al., 2014) and projector system with a schematic showing the structure of the barrel, projectile, sabot, and explosive chamber (Sawada et al., 2017). **(b)** Schematic of the shooting operation of the projector system showing (1) the explosion, (2) acceleration, and

(3) shot of the projectile.

Figure 2. Chemical structure of the nitrocellulose and lead (II) thiocyanate in the KTB and RK ignition charge explosives.

Figure 3. Apparatus and configuration of the laboratory-based projector system at the Institute of Space and Astronautical Science (ISAS), Sagamihara, in March 2015; **(a)** upper part of the projectile chamber, **(b)** explosive chamber, **(c)** interior of the projectile chamber, **(d, e)** gas sample cylinders, and **(f)** schematic of the entire simulation.

Figure 4. (a, b) Carbonaceous soot products after the explosion. **(c)** Volatile gas sample cylinder.

Figure 5. GC/MS chromatograms showing the volatile gases (methane, carbon dioxide, ethene, ethane, hydrogen sulfide, propane, benzene, and toluene) from the quenched carbonaceous product (w/o sabot). TIC stands for total ion chromatogram.

Figure 6. TD-GC/MS chromatograms of **(a)** the aliphatic molecules (*n*-alkanes); **(b–e)** aromatic molecules (e.g., monocyclic species: benzene, toluene, ethyl benzene, xylene, and phenol; bicyclic species: naphthalene, methyl naphthalene, dimethyl-naphthalene, and biphenyl; tricyclic species: phenanthrene, anthracene, methyl phenanthrene; and tetracyclic species: fluoranthene and pyrene); **(f)** heterocyclic molecules (e.g., dibenzofuran) from the quenched carbonaceous product without the sabot system (w/o sabot). Please see also Figure 7 for a comparison of PAH profiles from the systems w/ or w/o the sabot.

Figure 7. The relationship between the number of rings of the PAHs and their relative

abundance normalized to benzene at 100. The abundance profiles were from benzene (monocyclic), naphthalene (bicyclic), phenanthrene (tricyclic), and pyrene (tetracyclic), where the concentrations of alkyl-PAHs were not included in the determination of each relative abundance.

Figure 8. μXRF surface imaging for representative elements (Fe, red; K, green; Al, blue; and Cl, light blue) for the carbonaceous soot products (the explosion experiment with the sabot). The white scale bar represents 2 mm.

Figure 9. (a) Optical microscopy image of the soot sample produced from the quenched carbonaceous product. **(b)** IR spectral signatures obtained from the red squares (#24, 26-28 are from white materials and #25 is from black material). Possible peak assignments with references (Socrates, 2004) are shown in Table 1.

Figure 10. IR peak intensity maps at (a) 860 cm^{-1} with baseline between 780-1060 cm^{-1}, (b) ~1000 cm^{-1} with baseline between 780-1060 cm^{-1}, (c) 1100 cm^{-1} with baseline between 1060-1140 cm^{-1}, (d) 1830 cm^{-1} with baseline between 1780-1860 cm^{-1}, (e) 940 cm^{-1} with baseline between 780-1060 cm^{-1}, (f) ~1410 cm^{-1} with baseline between 1250-1750 cm^{-1}, (g) ~1520 cm^{-1} with baseline between 1250-1750 cm^{-1}, and (h) ~1640 cm^{-1} with baseline between 1250-1750 cm^{-1}.

Figure 11. Raman spectra of the soot sample recovered from the quenched carbonaceous product. "Black" indicates the spectra obtained from the black materials, and "white" indicates the spectra obtained from the white materials.

Table 1. Tentative peak assignments for the IR and Raman spectra based on Socrates (2004). The IR peaks with * are distributed in the right area, and the peaks with ** are distributed in the IR map (Figure 10).

	Wavenumber/cm^{-1}	**Functional groups**
IR	~3400	O-H, N-H
	1830 *	NOX (X = halogen), carbonate
	1640 **	H_2O, C=C, C=O (amide I)
	1520-10 **	C=C, NH_3^+, N-H (amide II)
	1420-10 **	CO_2^-, NH_4^+, NO_3^-, C-N (amide III), CO_3^{2-} (carbonate)
	1100 *	C-O, S=O
	1000 *	S=O
	940 **	N-O
	860 *	NO_3^-, carbonate
Raman	123	Unknown
	157-167	Carbonate
	202	Carbonate
	235	Unknown
	278	CCl, aromatic, carbonate
	553-573	CCl, aromatic, amide, C=O, C-S
	726	CCl, aromatic, amide, C-S, carbonate
	1095	NO_3^-, aromatic, C-O, C-N, S=O, carbonate
	1475-1490	NH_3^+, aromatic, pyrrole, carbonate
	1729	C=O

(a)

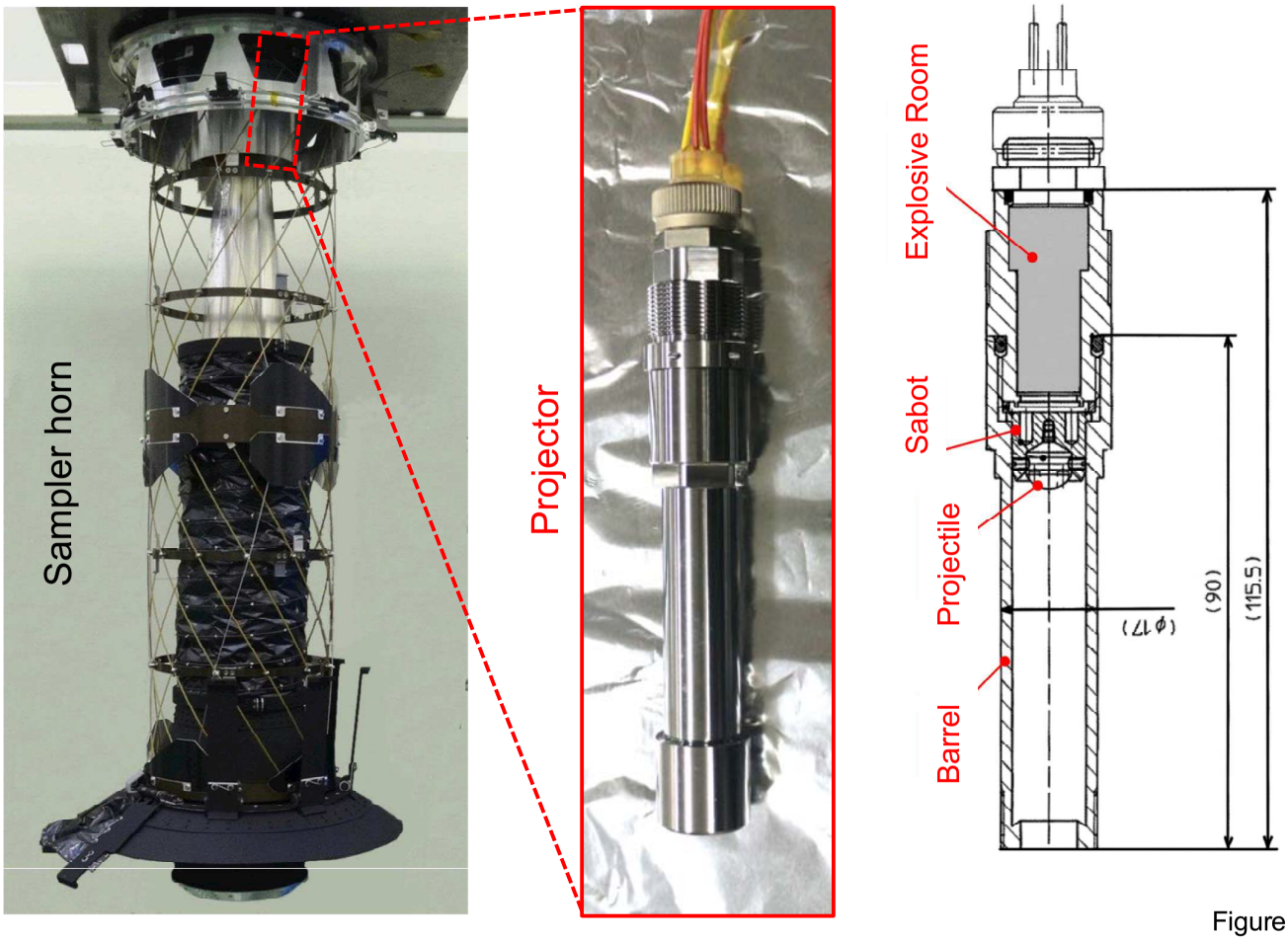

Figure 1

(b)

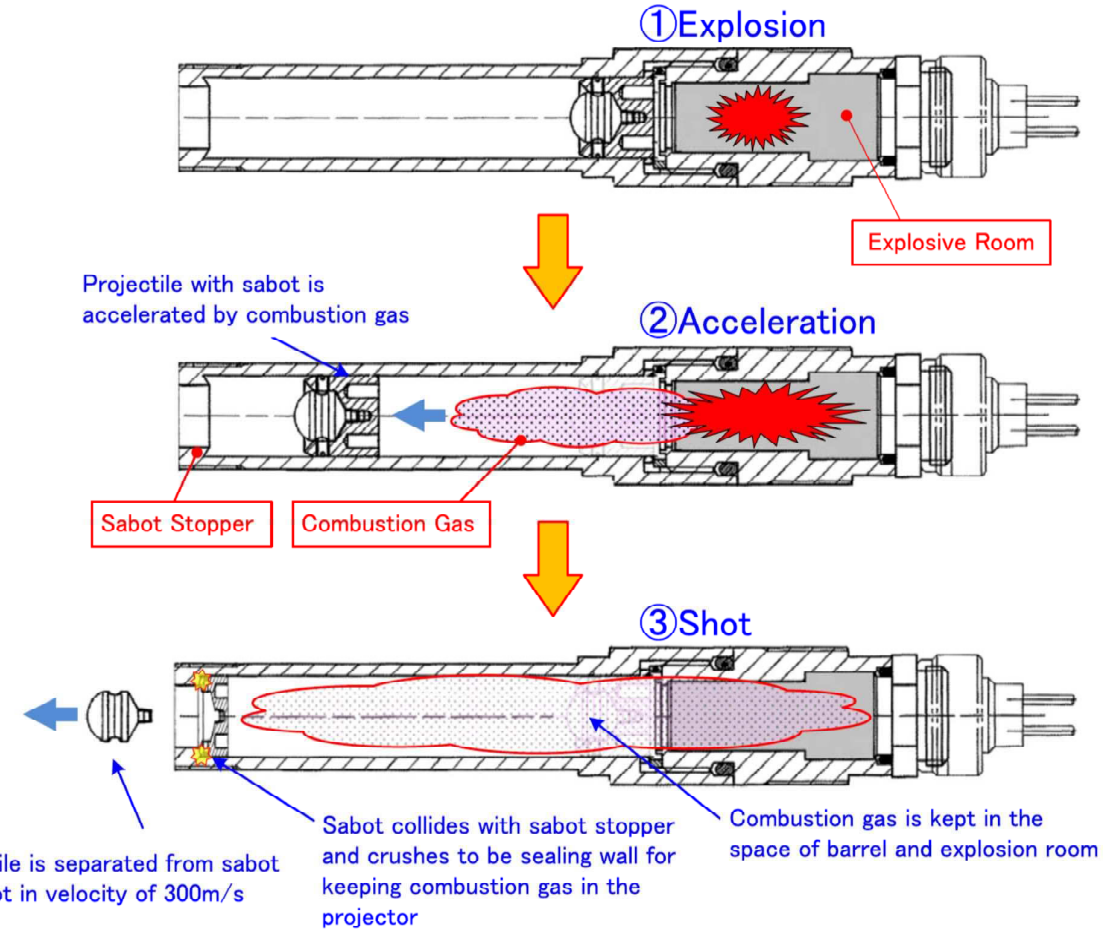

Figure 1

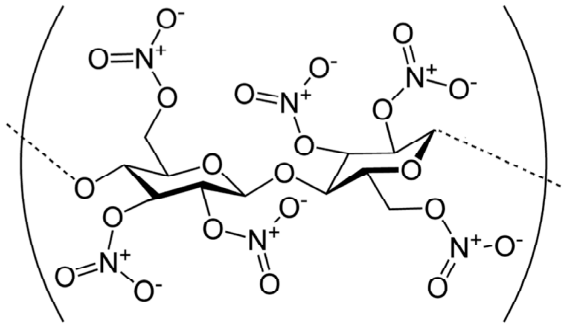

Nitrocellulose

Chemical Formula: $[C_6H_7(NO_2)_3O_5]n$

Flash point: 4.4°C

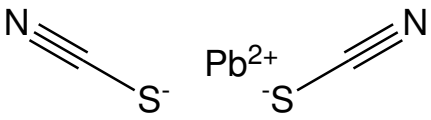

Lead (II) thiocyanate

Chemical Formula: $Pb(SCN)_2$

Exact Mass: 323.93

Molecular Weight: 323.36

Figure 2

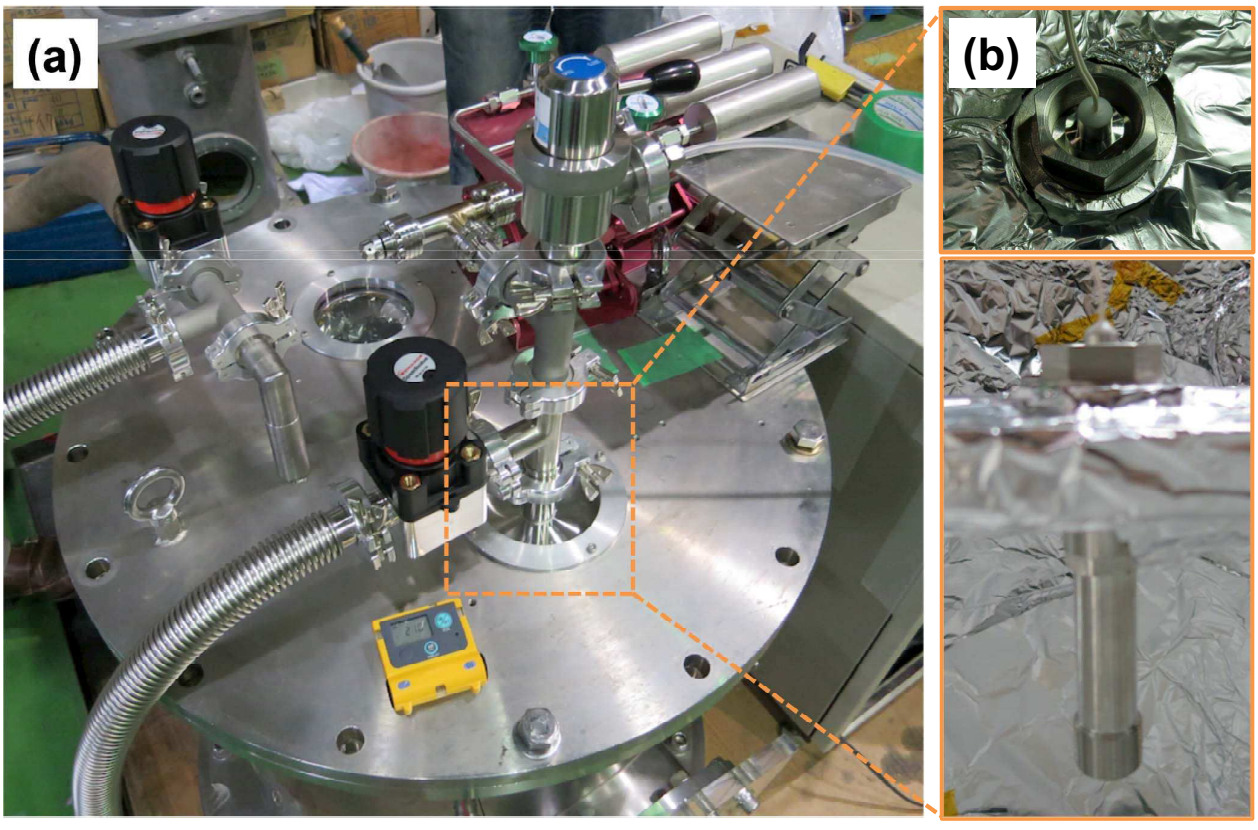

Figure 3

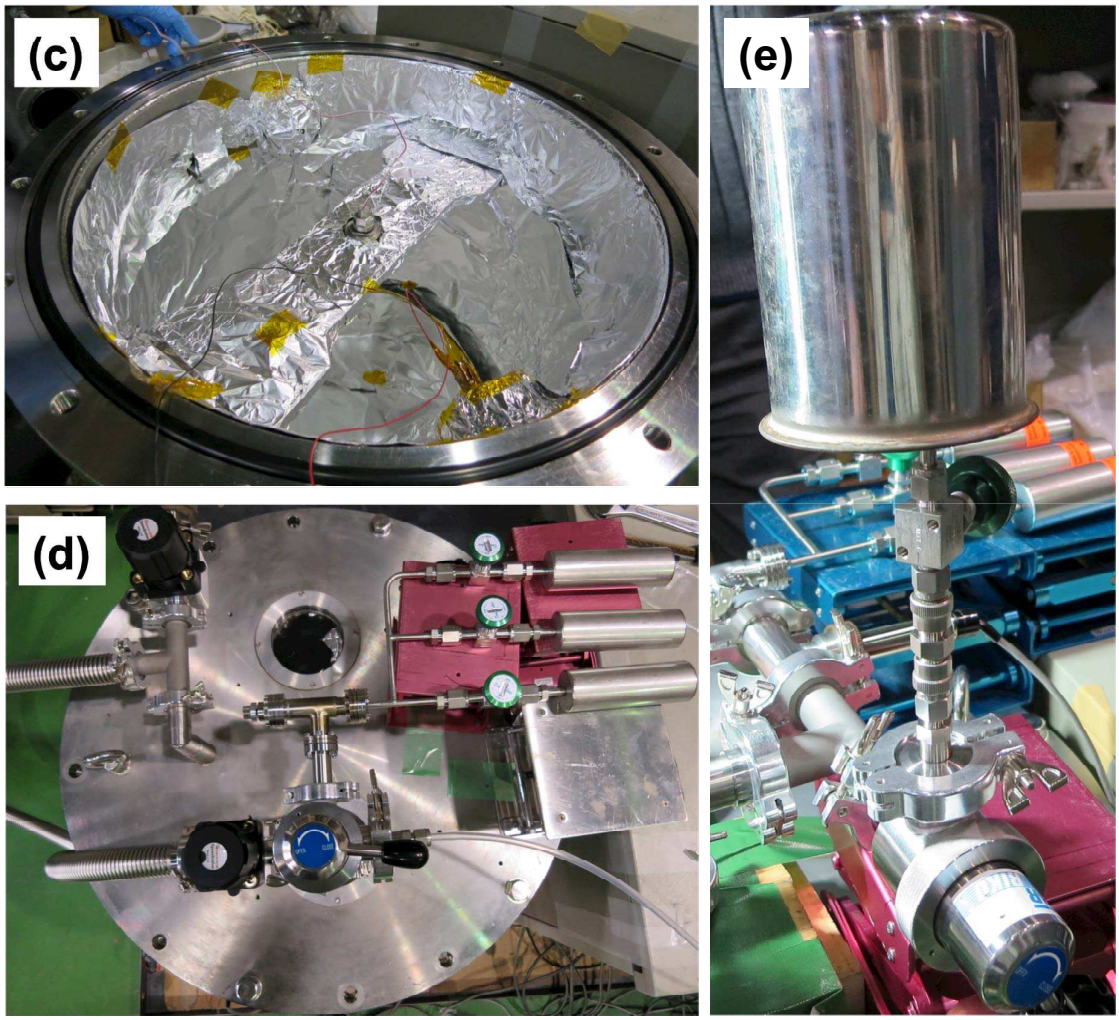

Figure 3

(f)

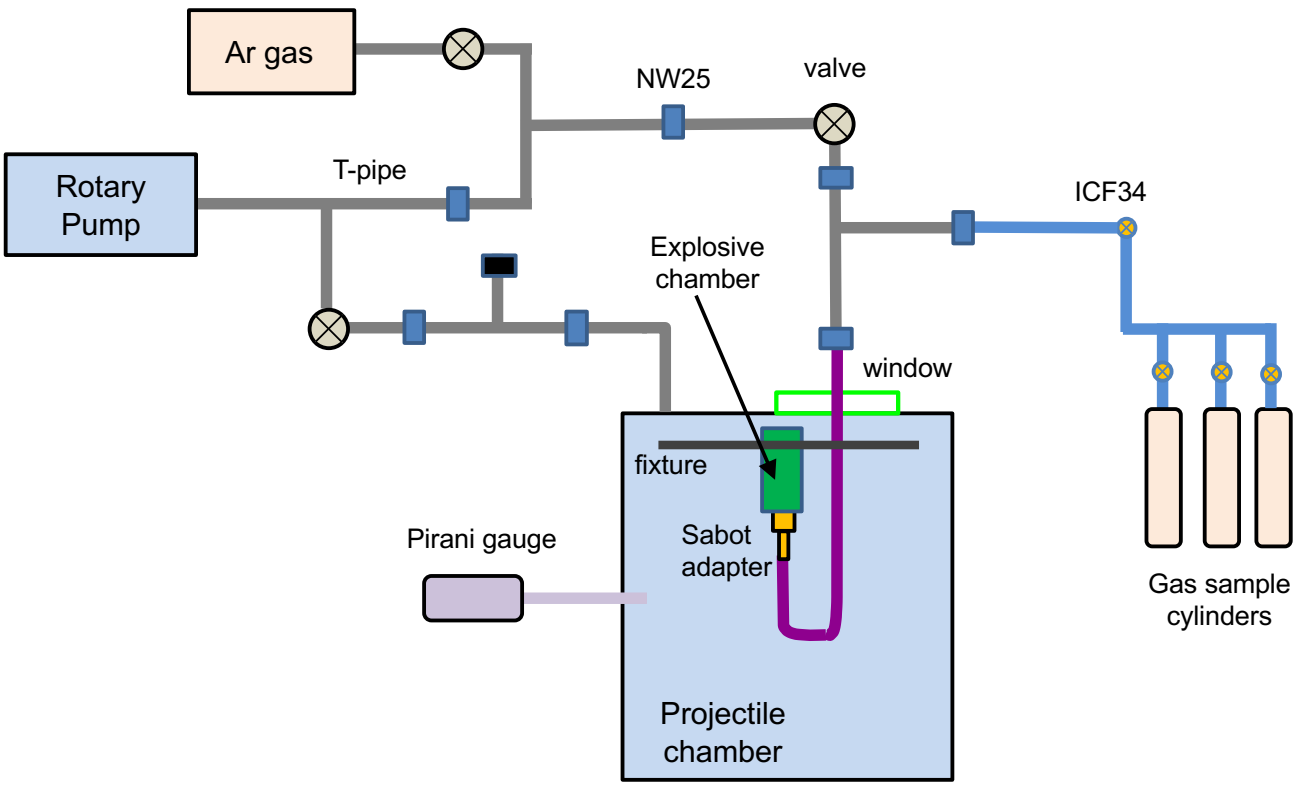

Figure 3

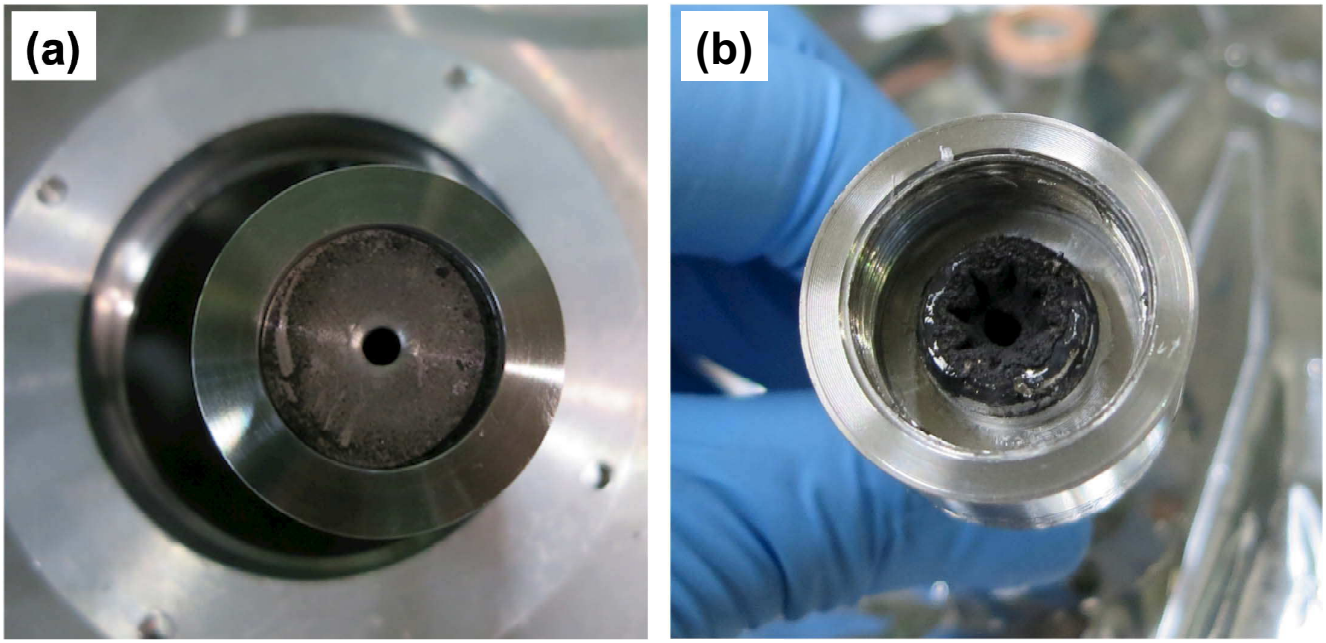

Figure 4

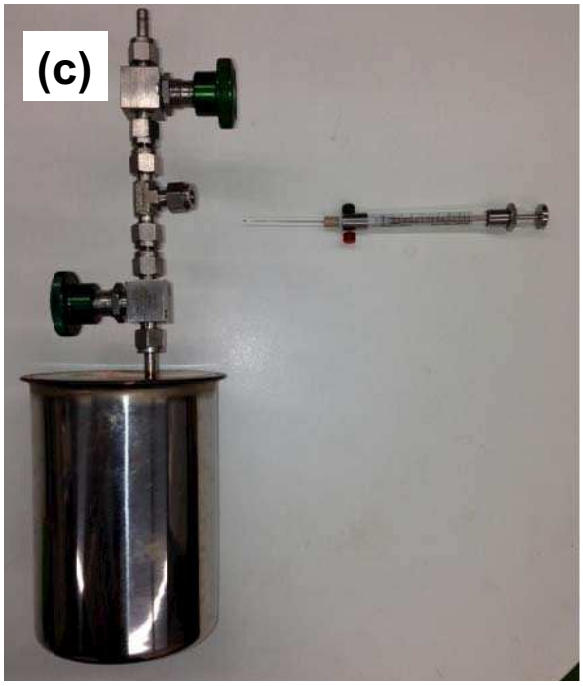

Figure 4

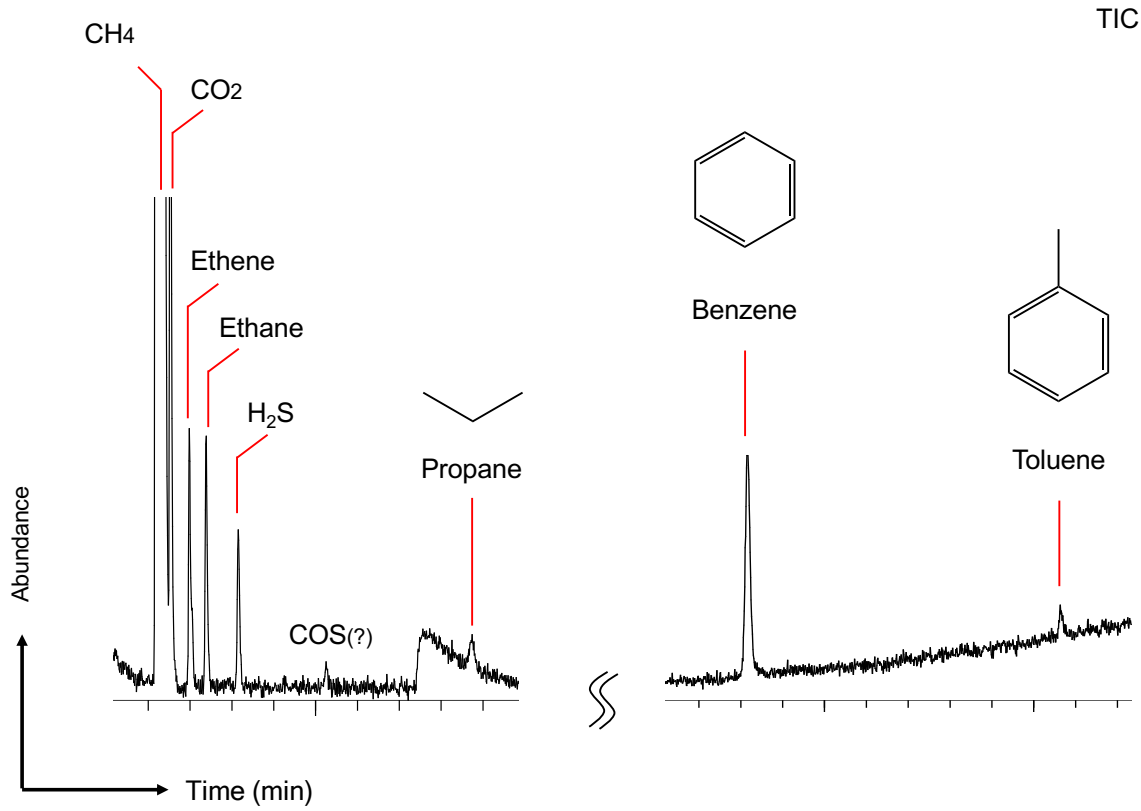

Figure 5

(a) Aliphatic molecules

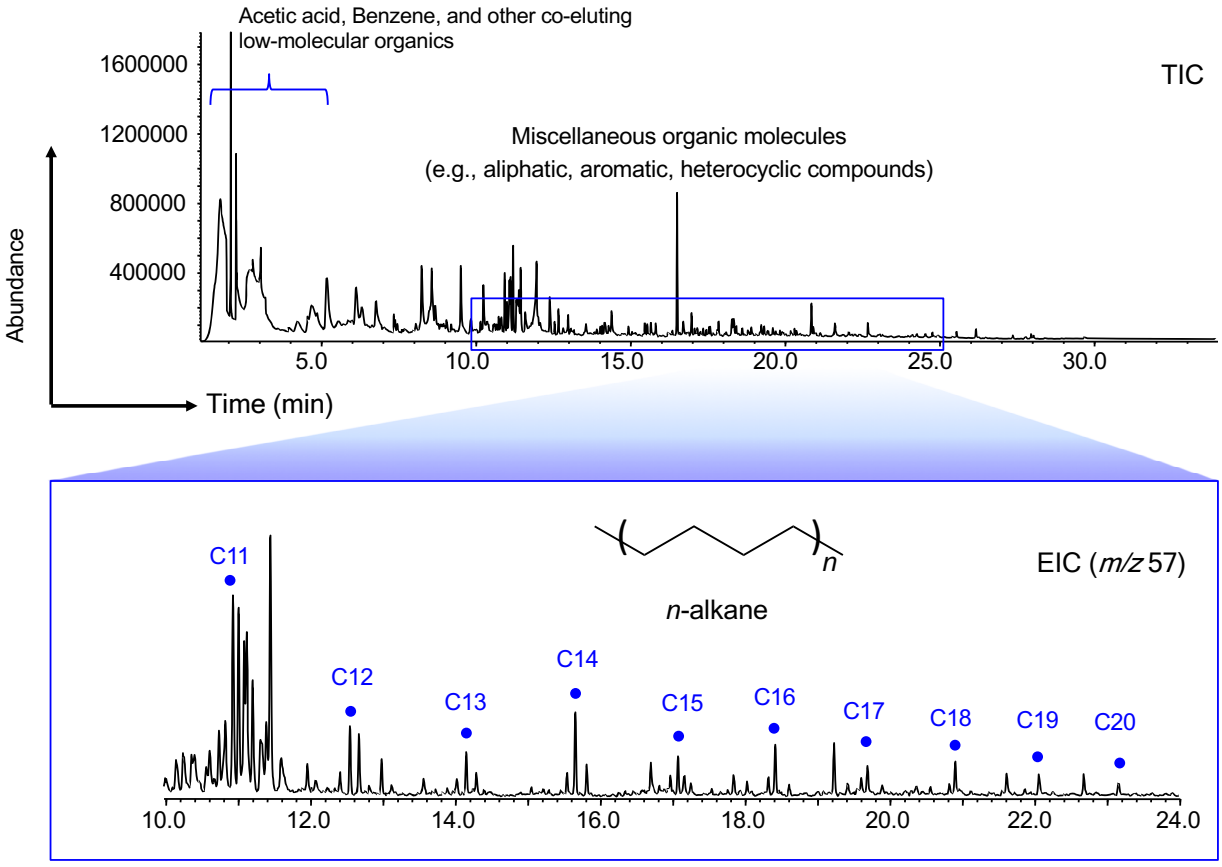

Figure 6

(b) Aromatic molecules: 1-Rings

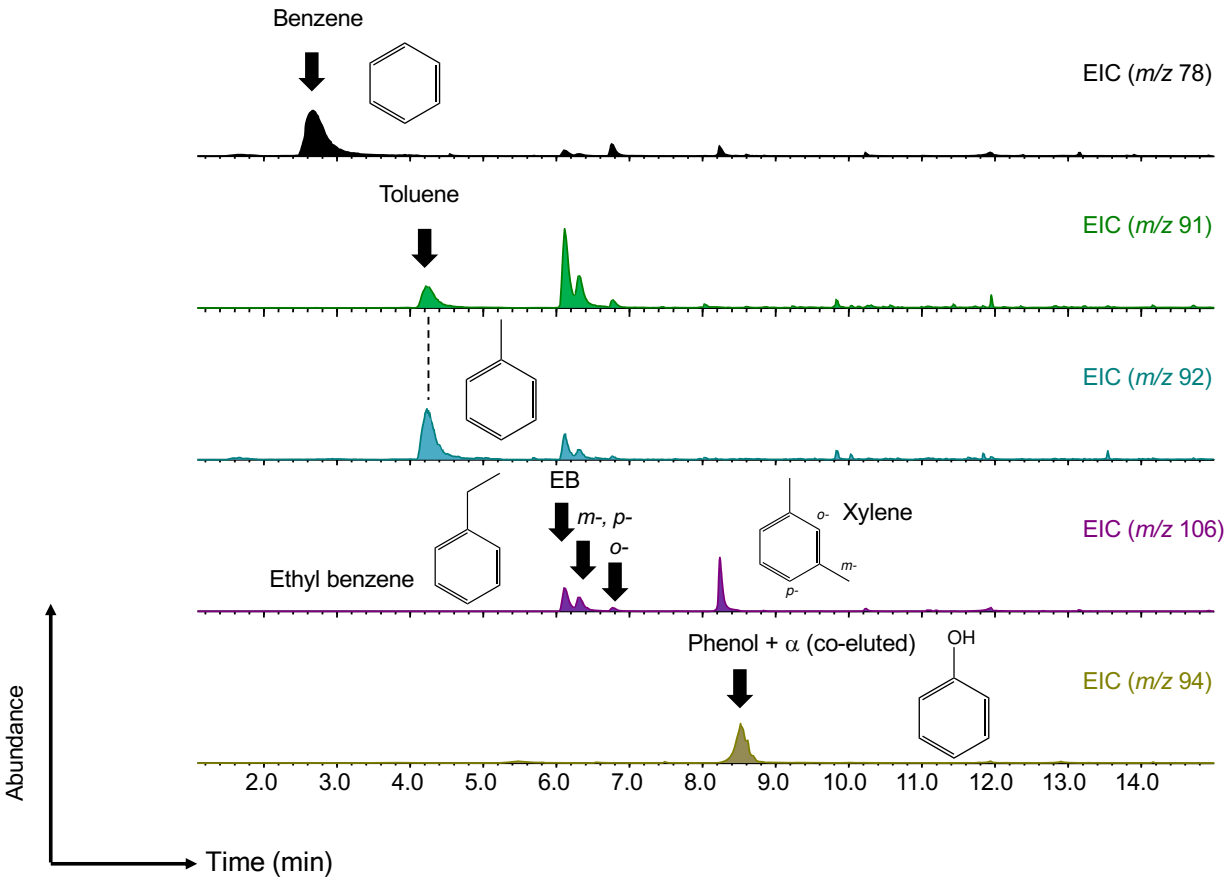

Figure 6

(c) Aromatic molecules: 2-Rings

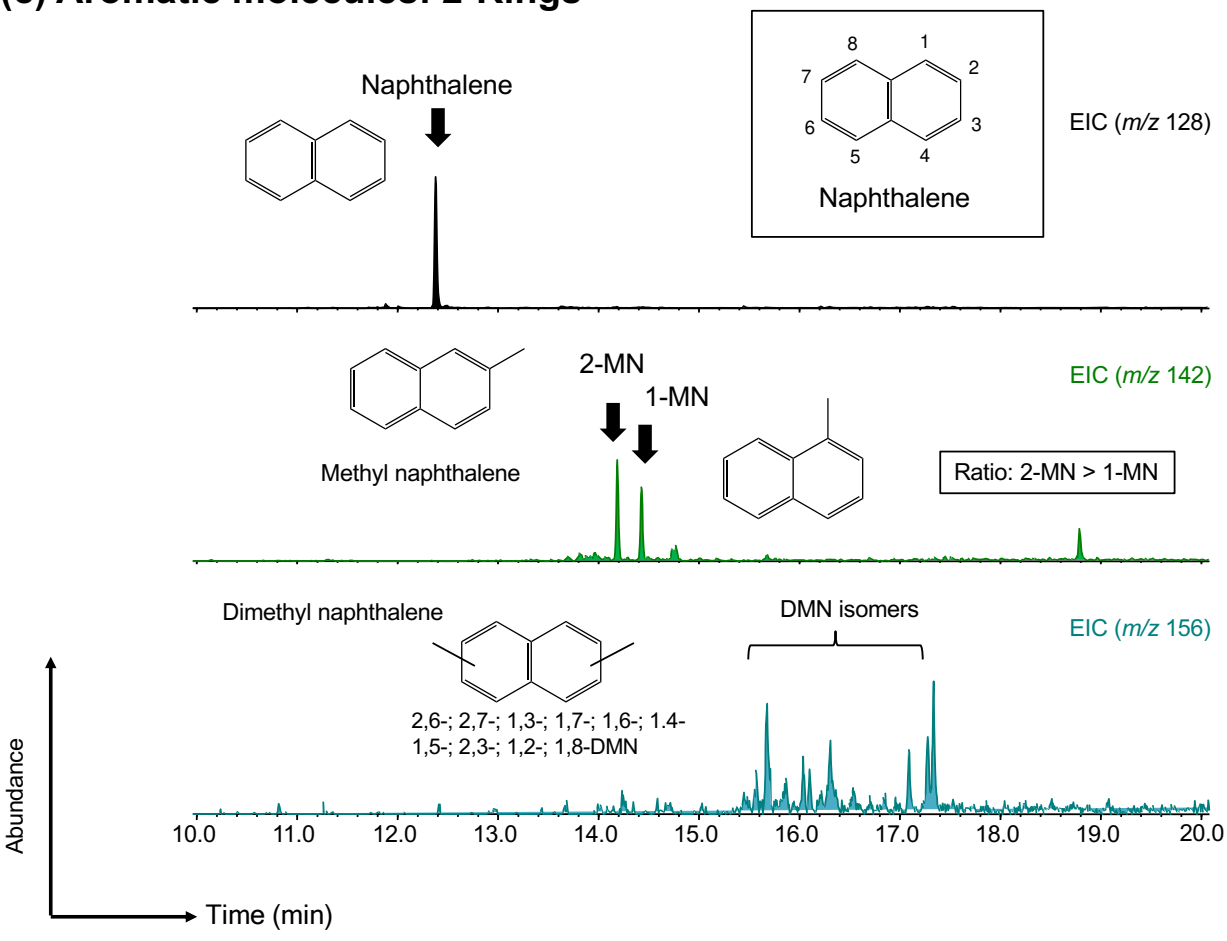

Figure 6

(d) Aromatic molecules: 2,3-Rings

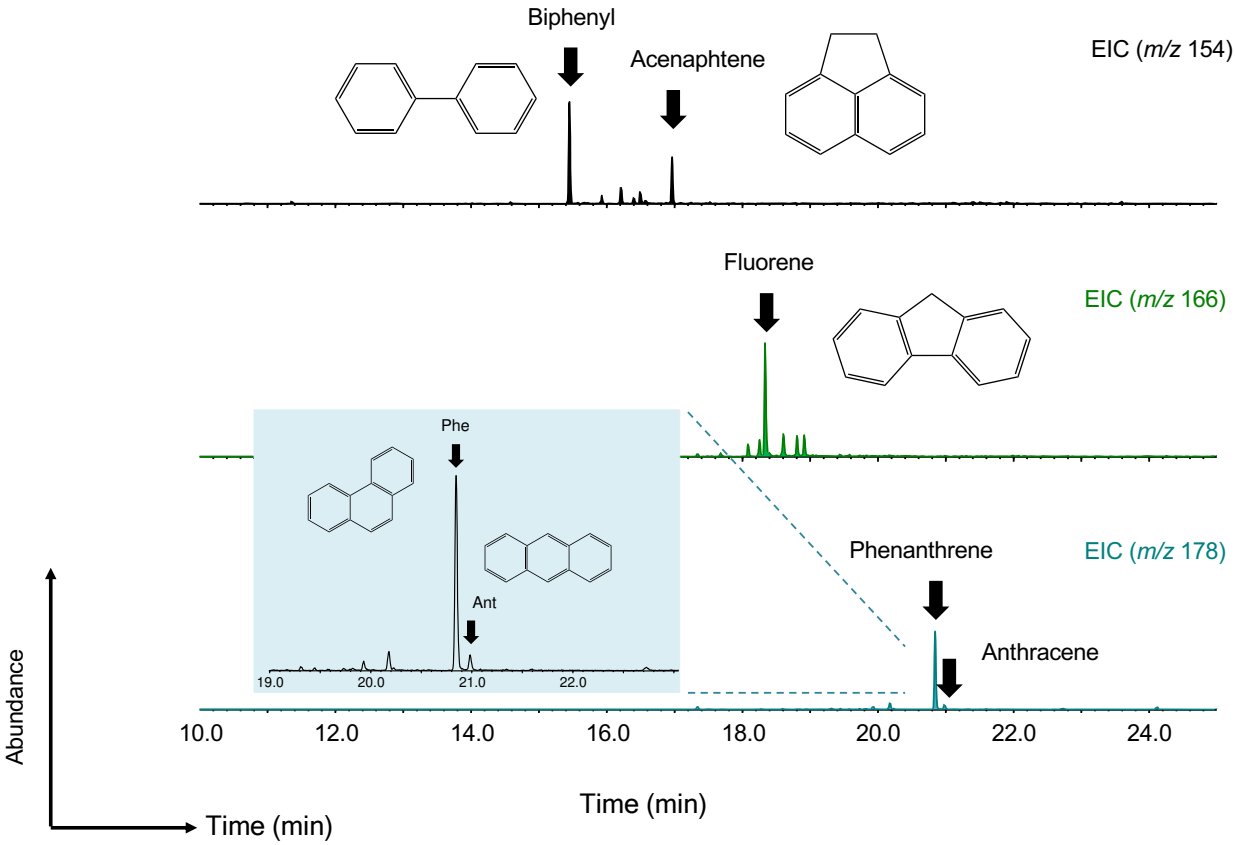

Figure 6

(e) Aromatic molecules: 3,4-Rings

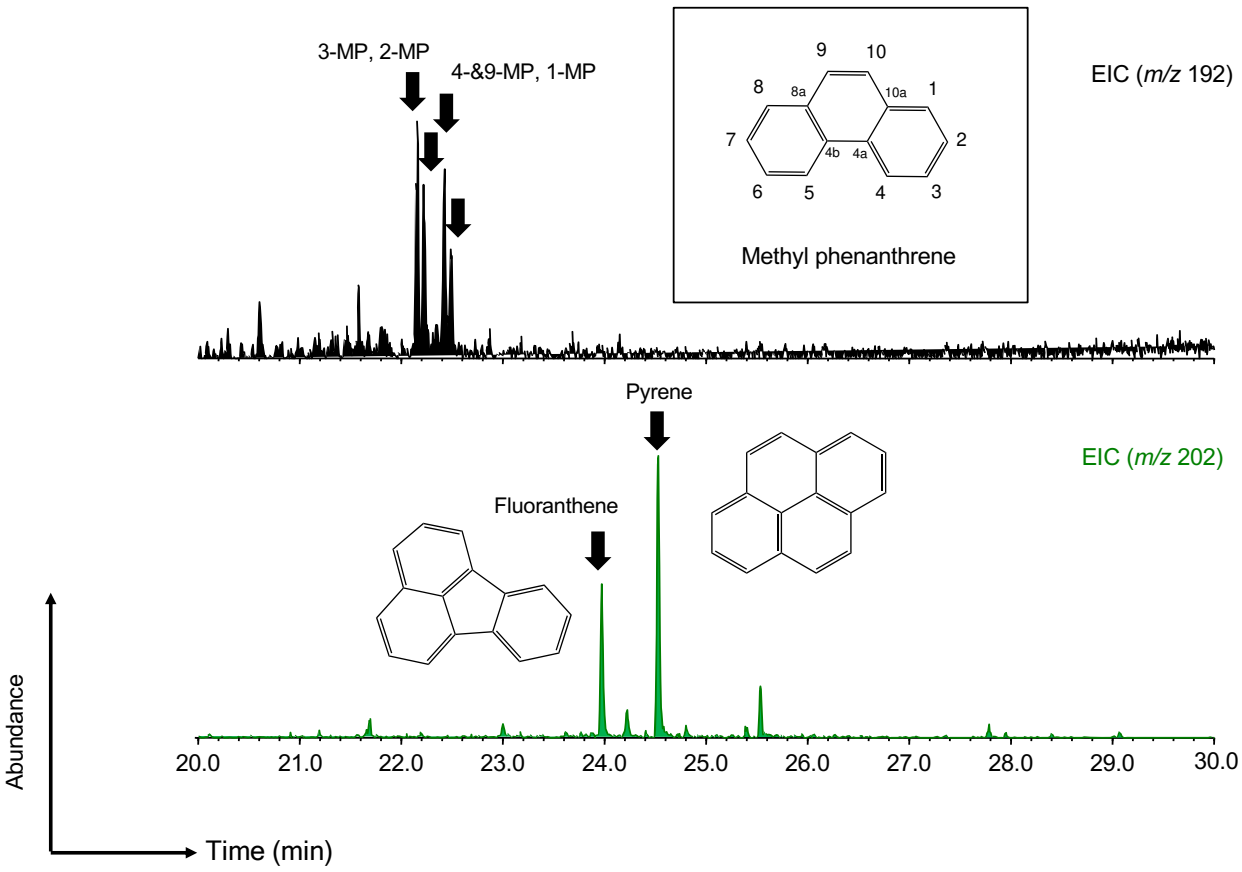

Figure 6

(f) Heterocyclic molecule

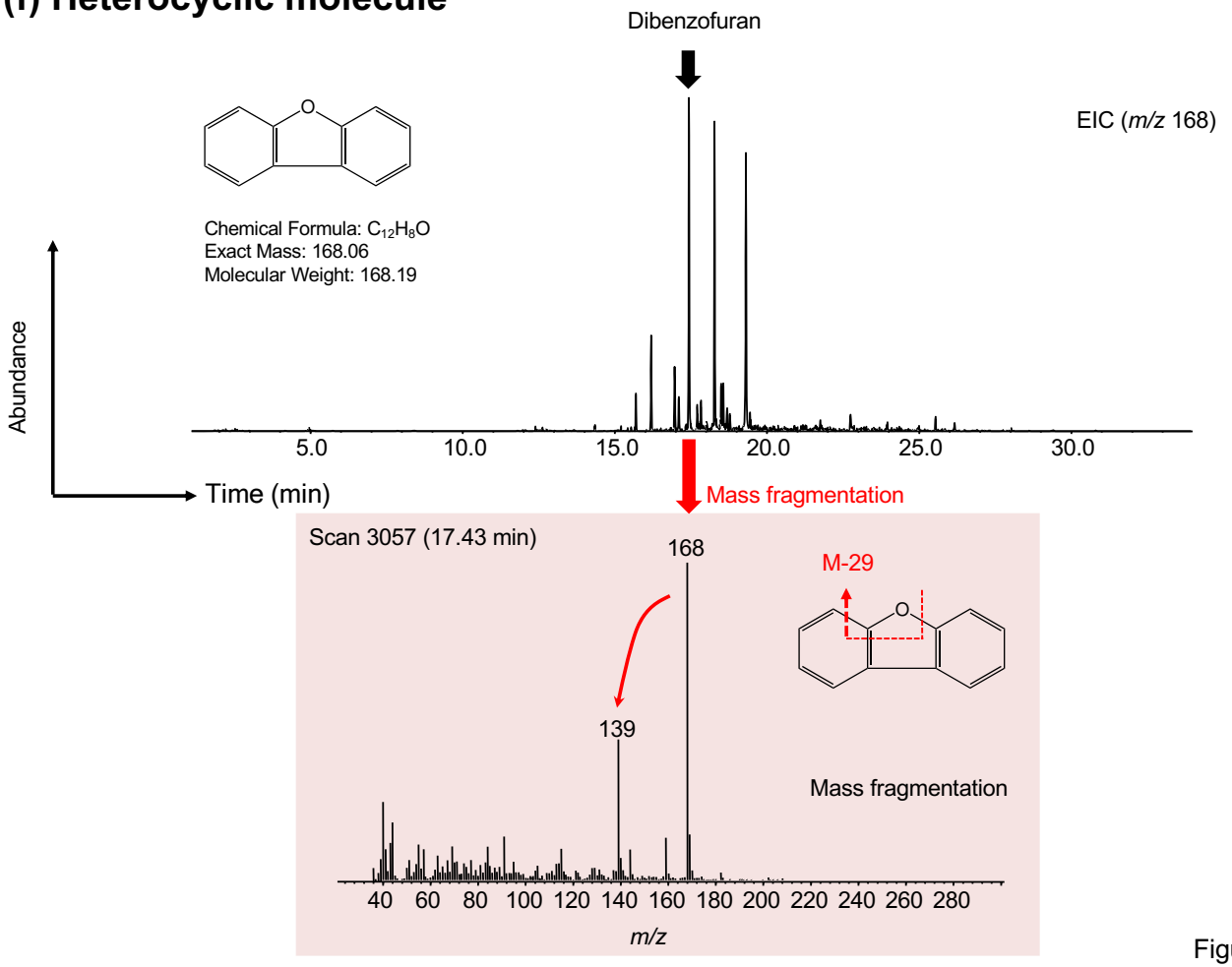

Figure 6

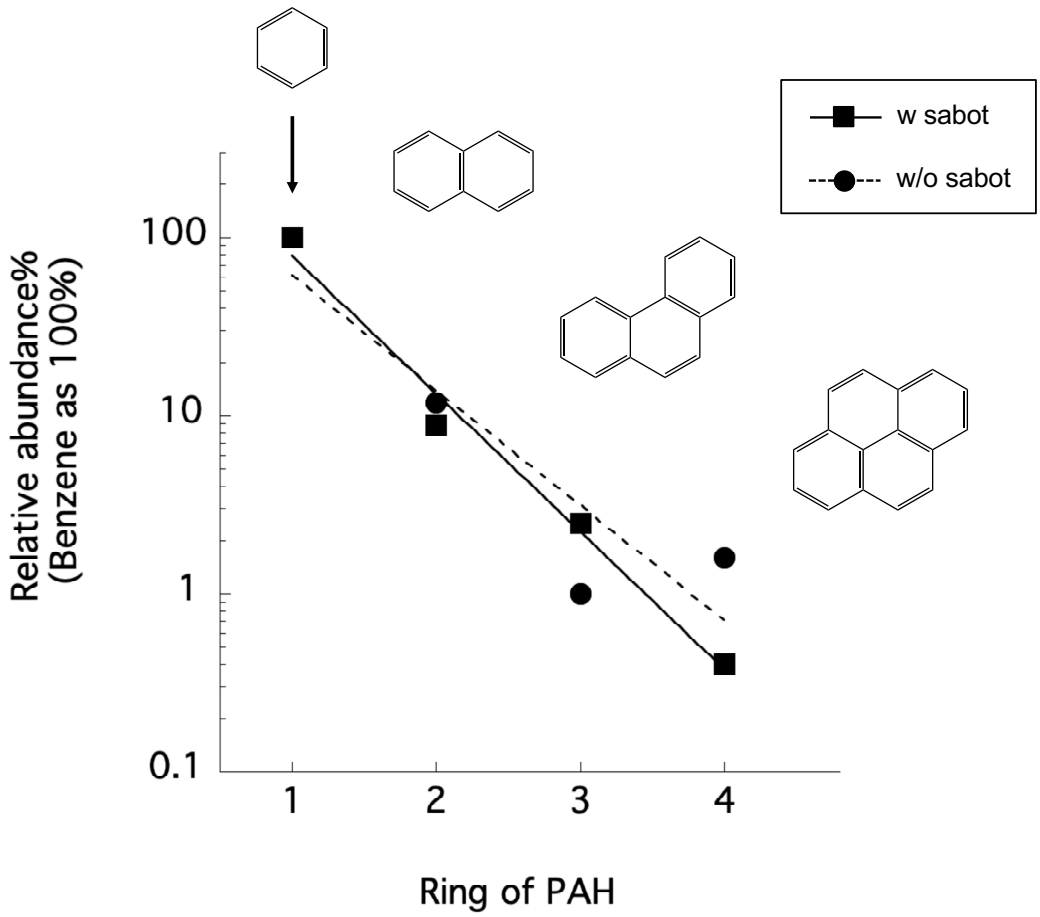

Figure 7

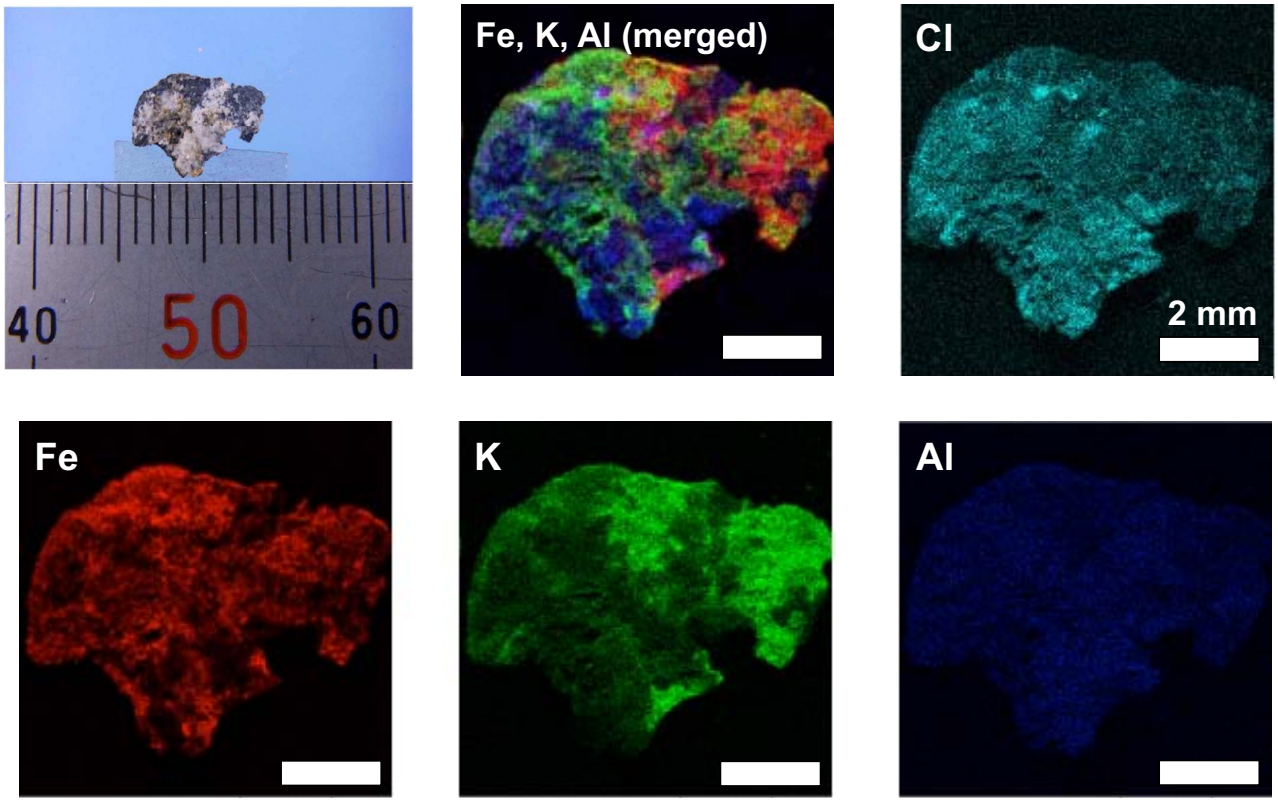

Figure 8

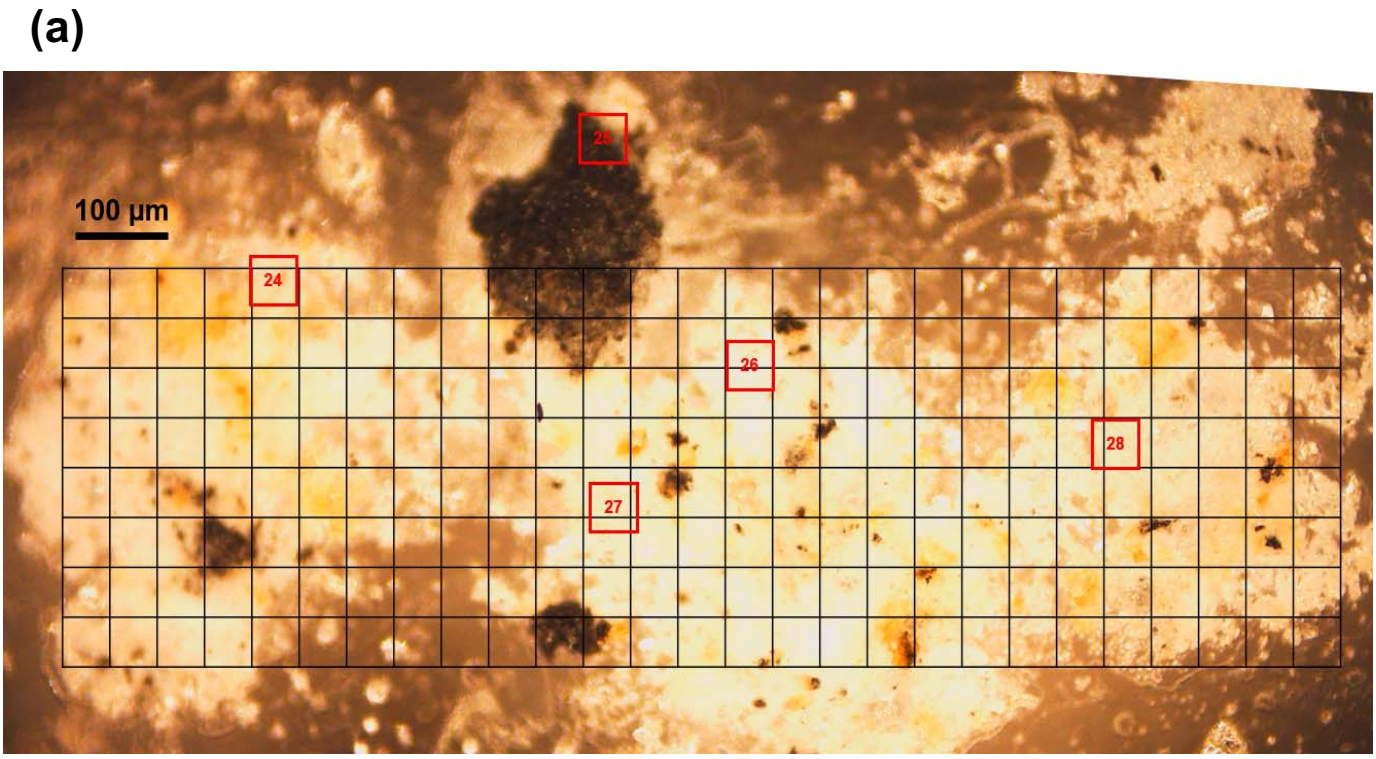

Figure 9

(b)

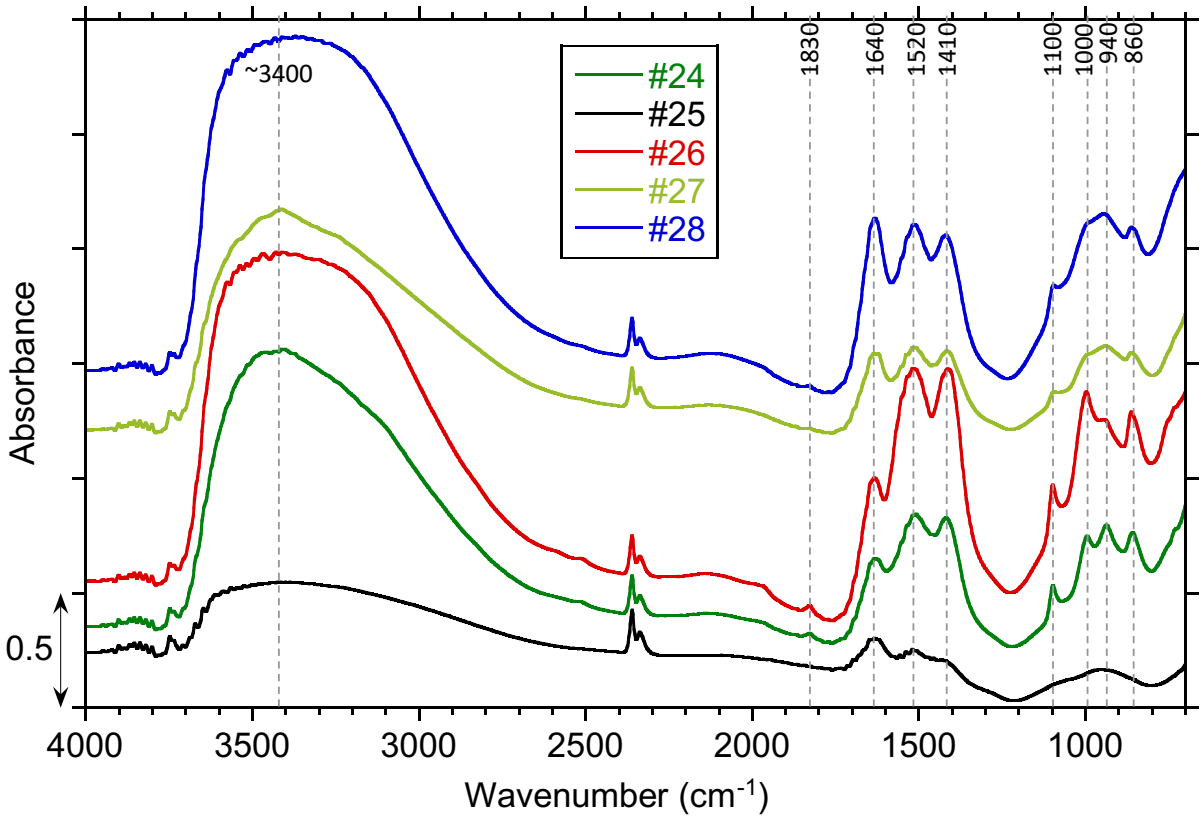

Figure 9

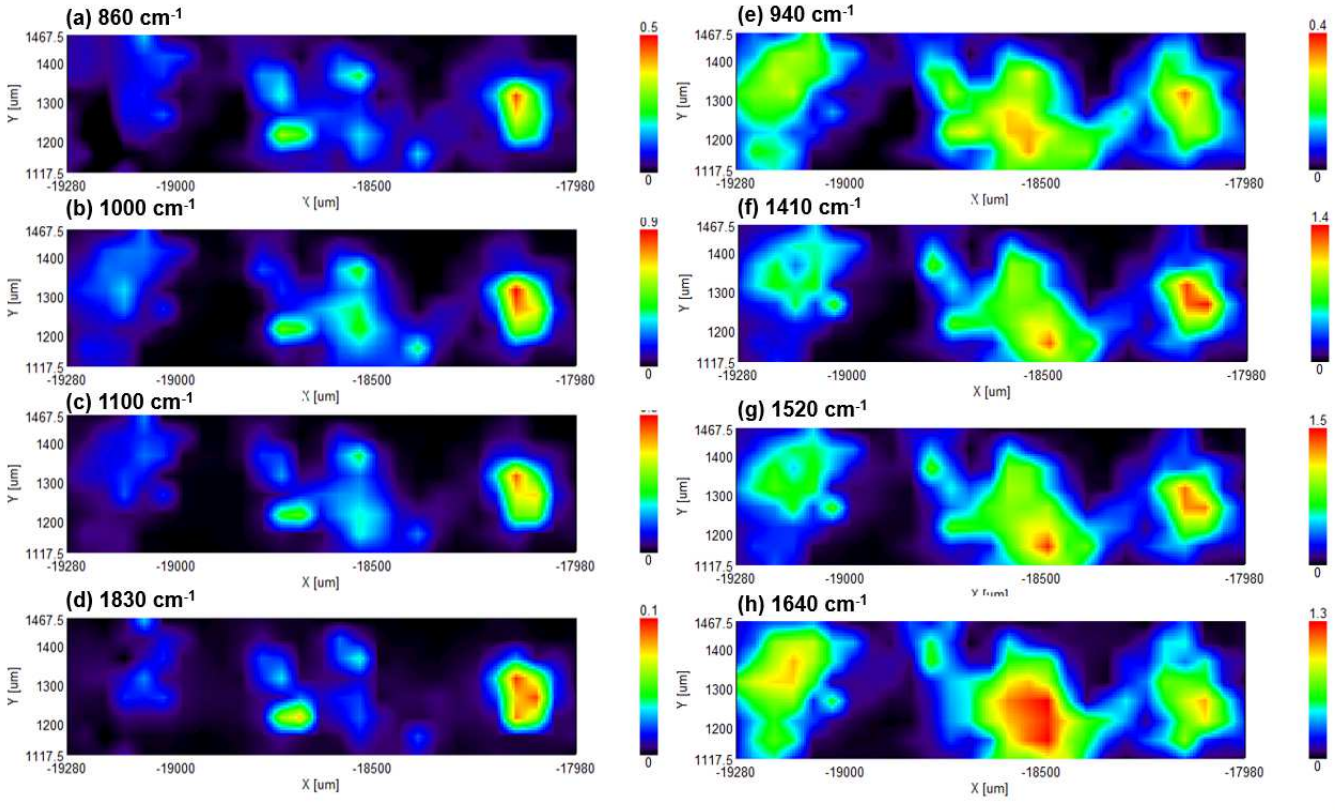

Figure 10

(a)

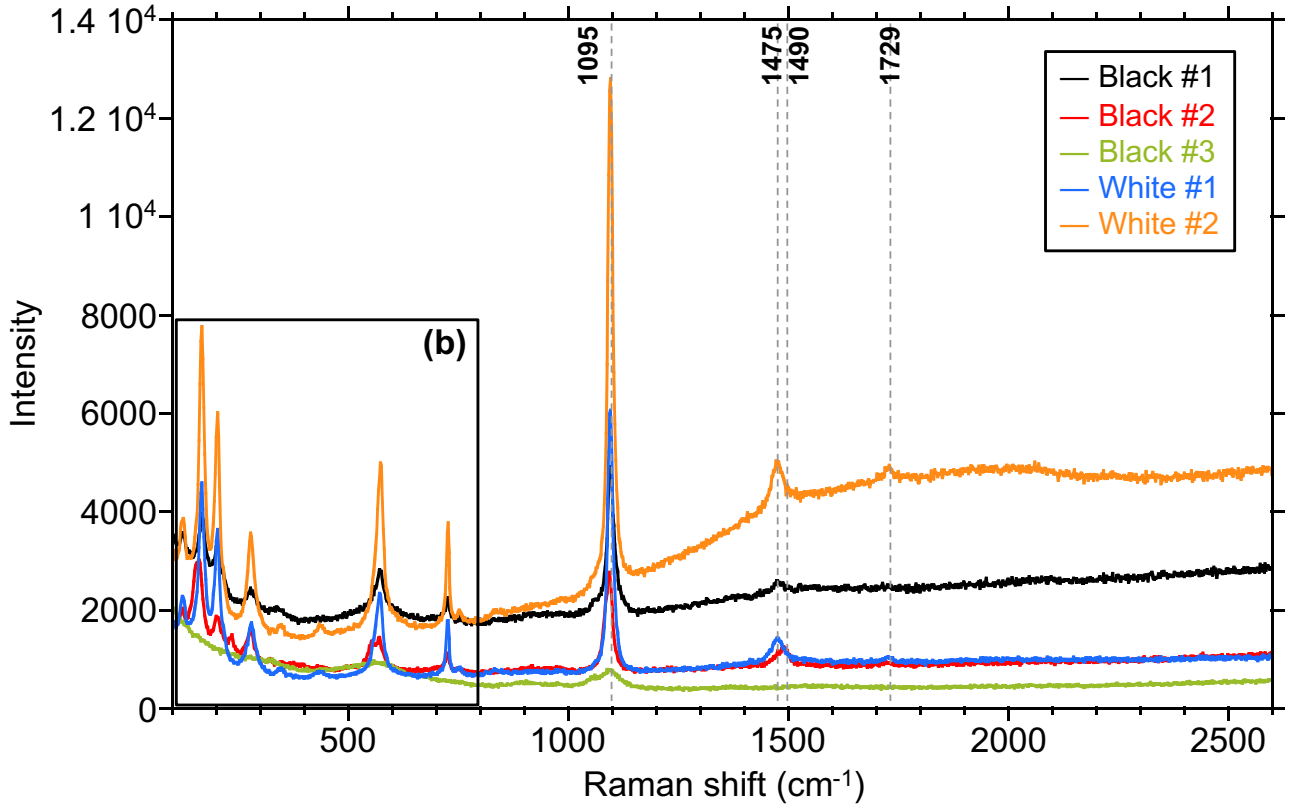

Figure 11

(b)

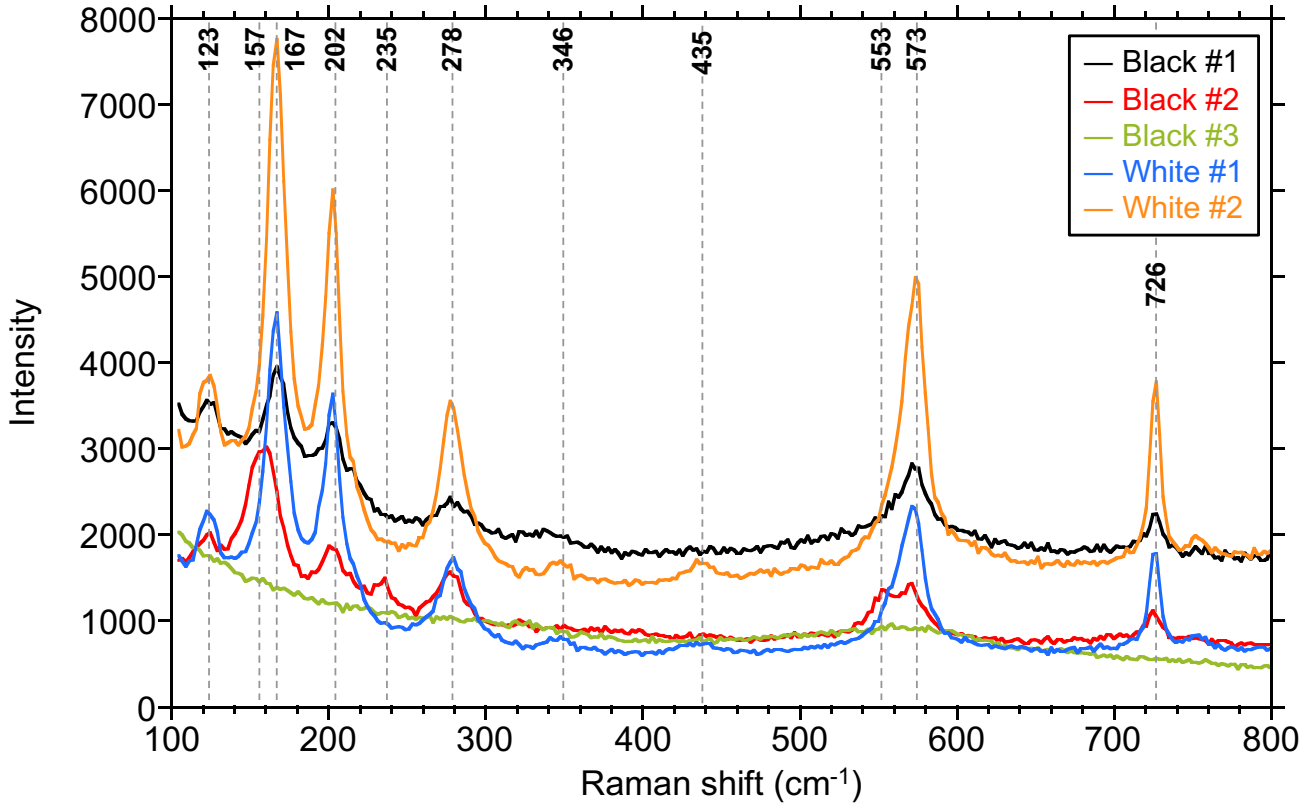

Figure 11

Figures

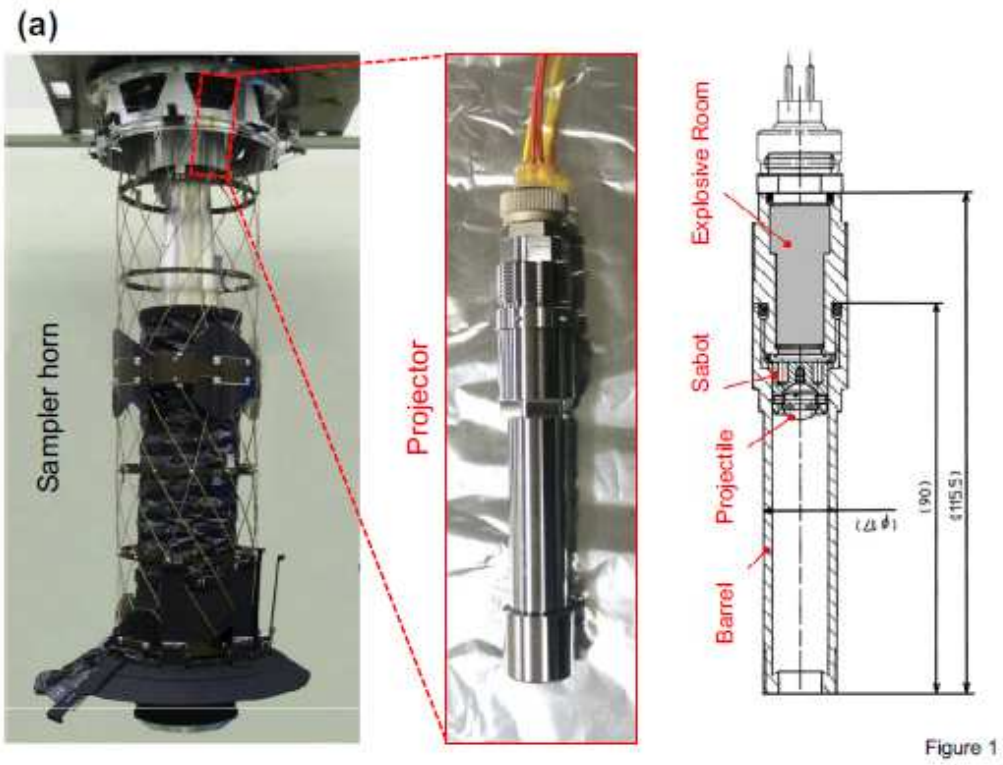

Figure 1

Figure 1

(a) Photograph of the Hayabusa2 sampler horn (Tachibana et al., 2014) and projector system with a schematic showing the structure of the barrel, projectile, sabot, and explosive chamber (Sawada et al.,

2017). (b) Schematic of the shooting operation of the projector system showing (1) the explosion, (2) acceleration, and (3) shot of the projectile.

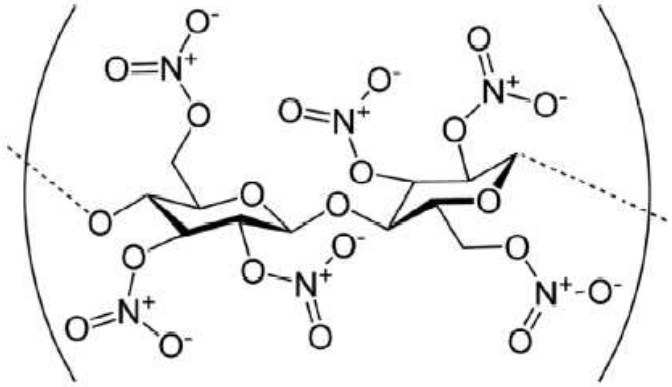

Nitrocellulose

Chemical Formula: $[C_6H_7(NO_2)_3O_5]n$

Flash point: 4.4°C

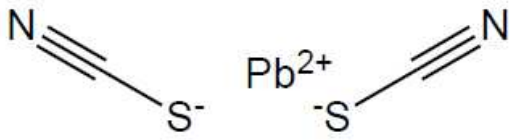

Lead (II) thiocyanate

Chemical Formula: $Pb(SCN)_2$

Exact Mass: 323.93

Molecular Weight: 323.36

Figure 2

Chemical structure of the nitrocellulose and lead (II) thiocyanate in the KTB and RK ignition charge explosives.

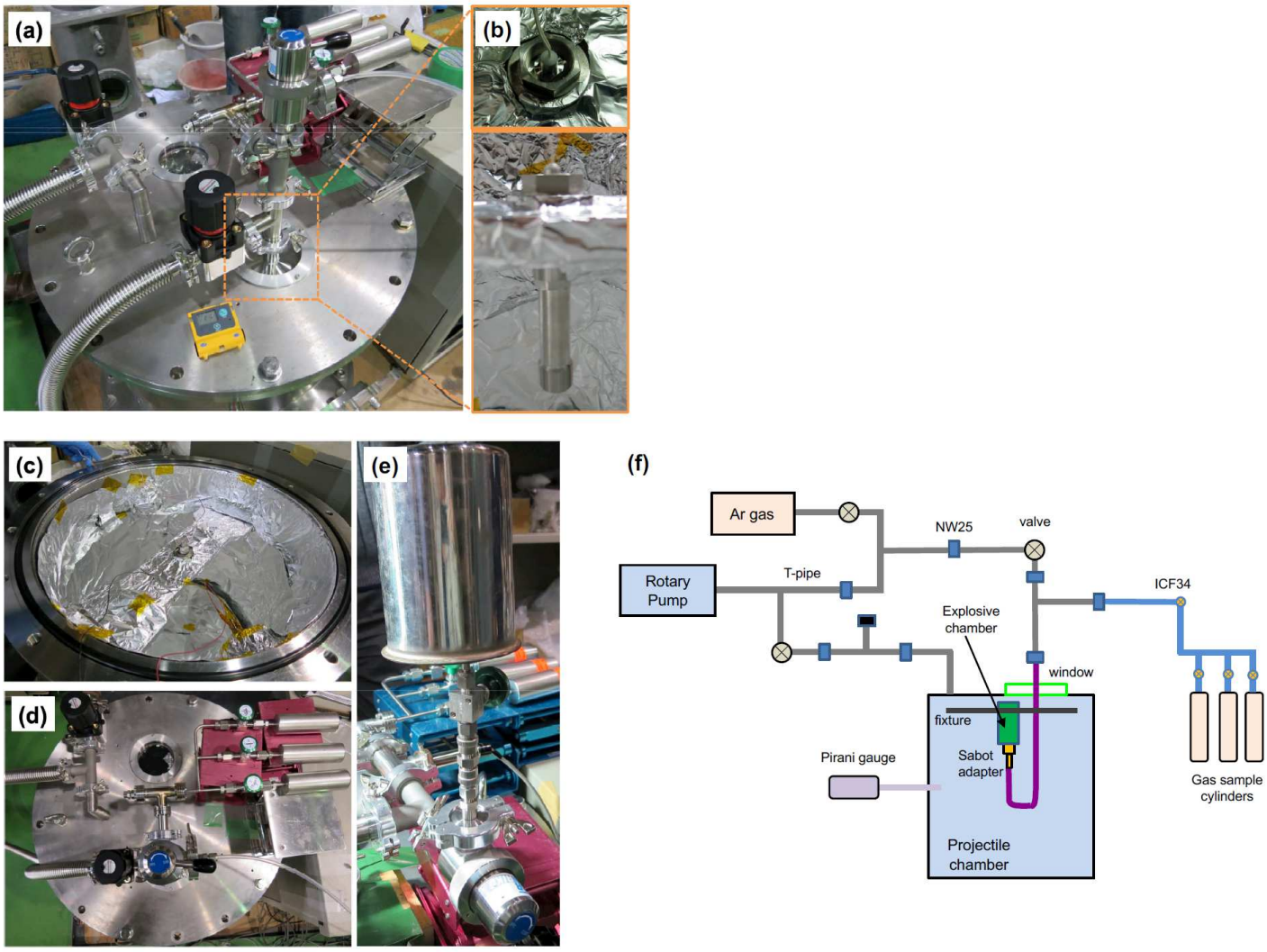

Figure 3

Apparatus and configuration of the laboratory-based projector system at the Institute of Space and Astronautical Science (ISAS), Sagamihara, in March 2015; (a) upper part of the projectile chamber, (b) explosive chamber, (c) interior of the projectile chamber, (d, e) gas sample cylinders, and (f) schematic of the entire simulation. The anomalous element profiles of metal (e.g., Aluminum) derived from the explosive chamber are potential indicators to trace the artifact if the sample has affected by off-nominal the projectile operation.

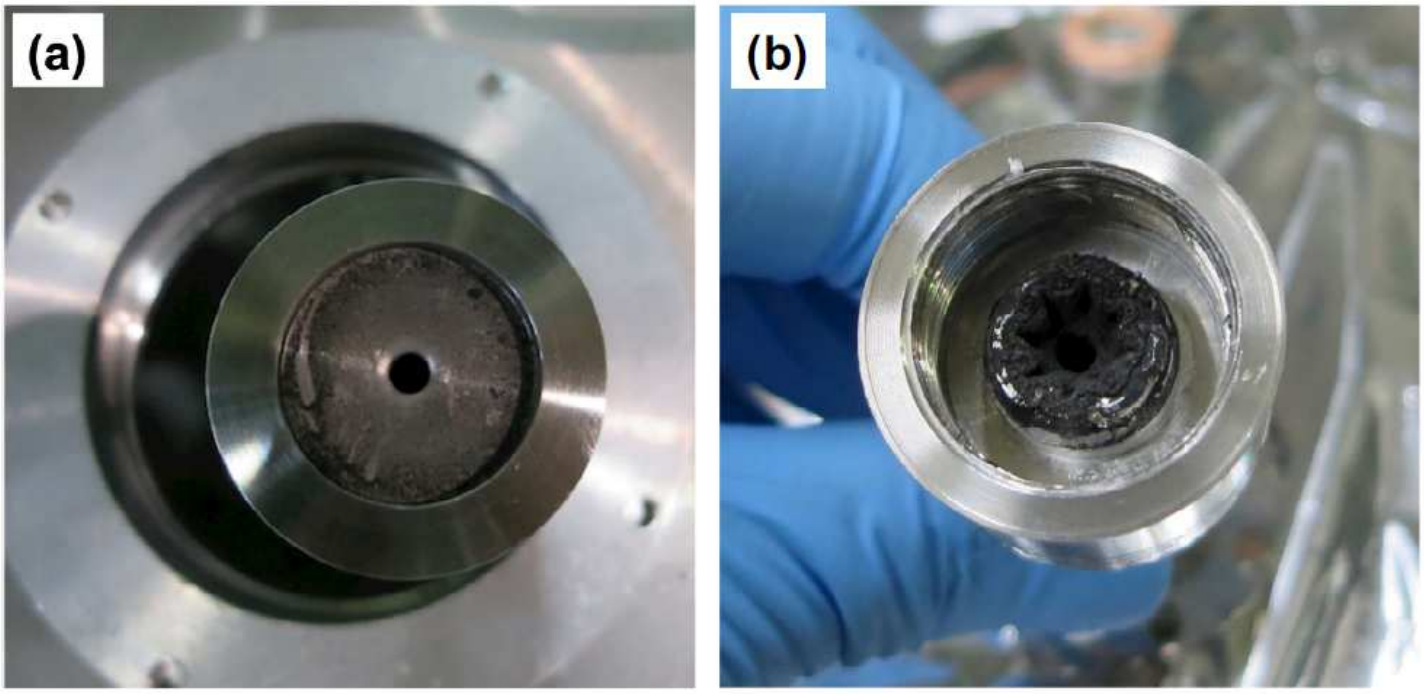

Figure 4

(a, b) Carbonaceous product after the explosion simulation. (c) Volatile gas sample cylinder.

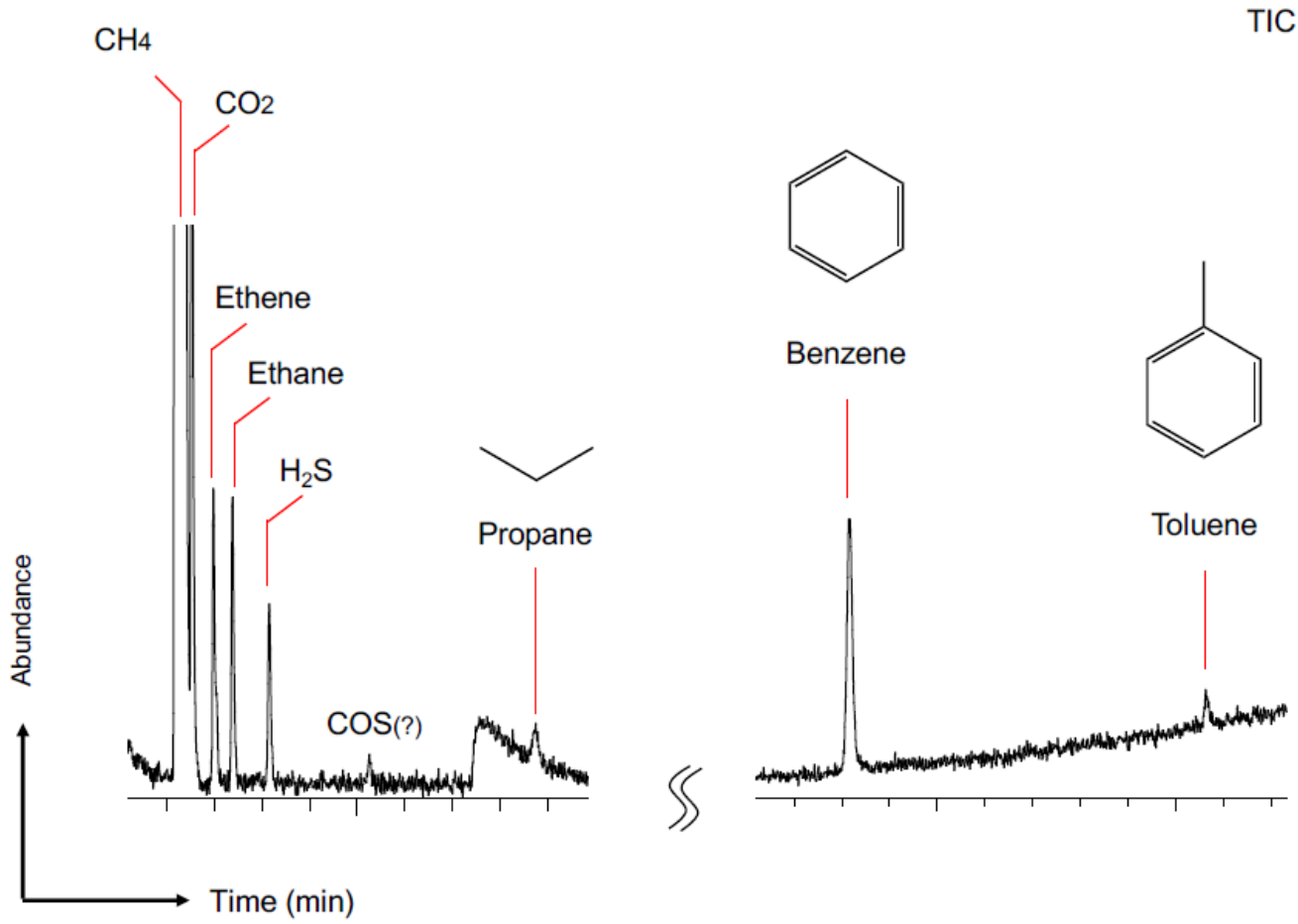

Figure 5

GC/MS chromatograms showing the volatile gases (methane, carbon dioxide, ethene, ethane, hydrogen sulfide, propane, benzene, and toluene) from the quenched carbonaceous product (w/o sabot). TIC stands for total ion chromatogram.

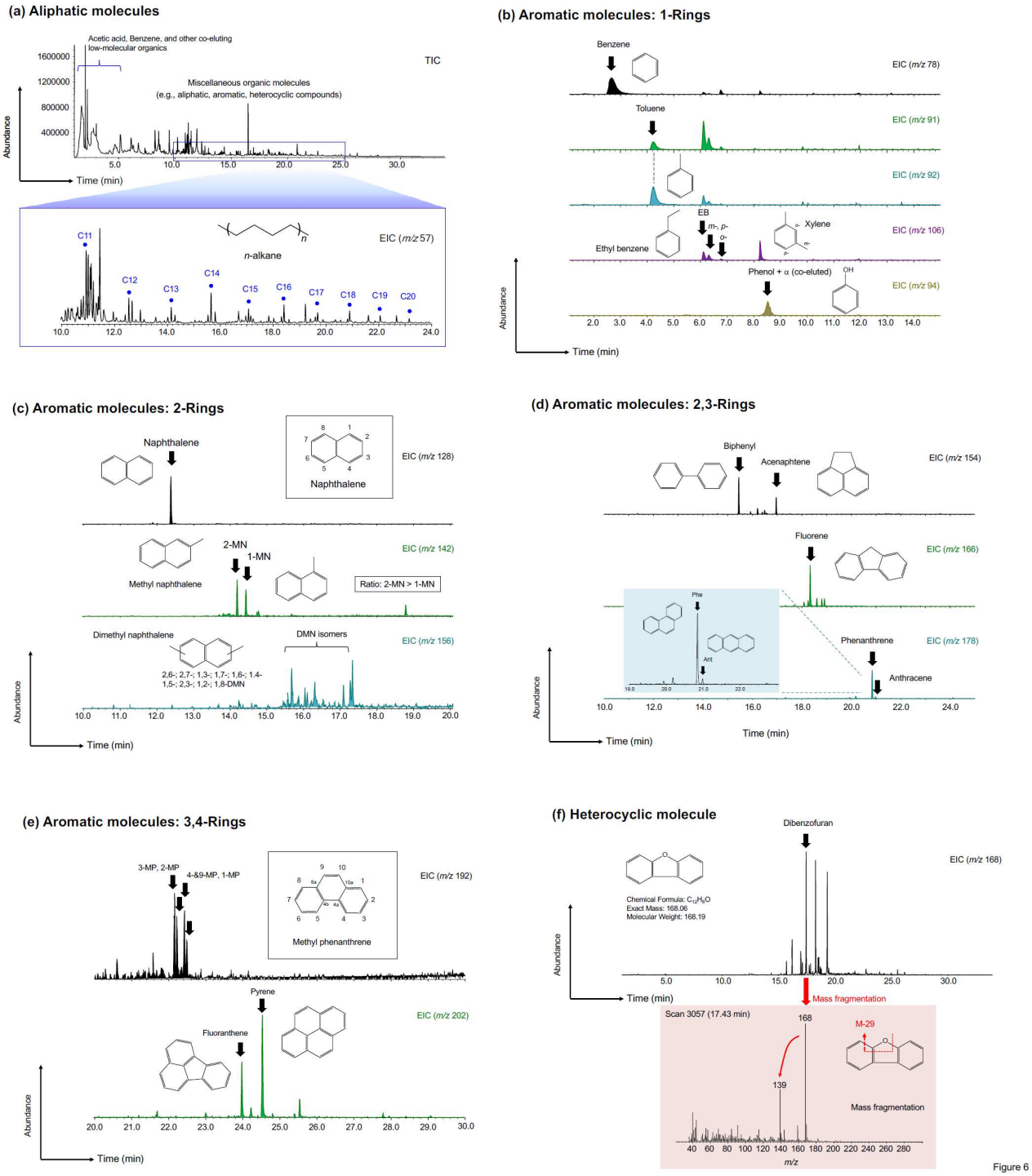

Figure 6

Figure 6

TD-GC/MS chromatograms of (a) the aliphatic molecules (n-alkanes); (b–e) aromatic molecules (e.g., monocyclic species: benzene, toluene, ethyl benzene, xylene, and phenol; bicyclic species: naphthalene, methyl naphthalene, dimethyl-naphthalene, and biphenyl; tricyclic species: phenanthrene, anthracene, methyl phenanthrene; and tetracyclic species: fluoranthene and pyrene); (f) heterocyclic molecules (e.g.,

dibenzofuran) from the quenched carbonaceous product without the sabot system (w/o sabot). Please see also Figure 7 for a comparison of PAH profiles from the systems w/ or w/o the sabot.

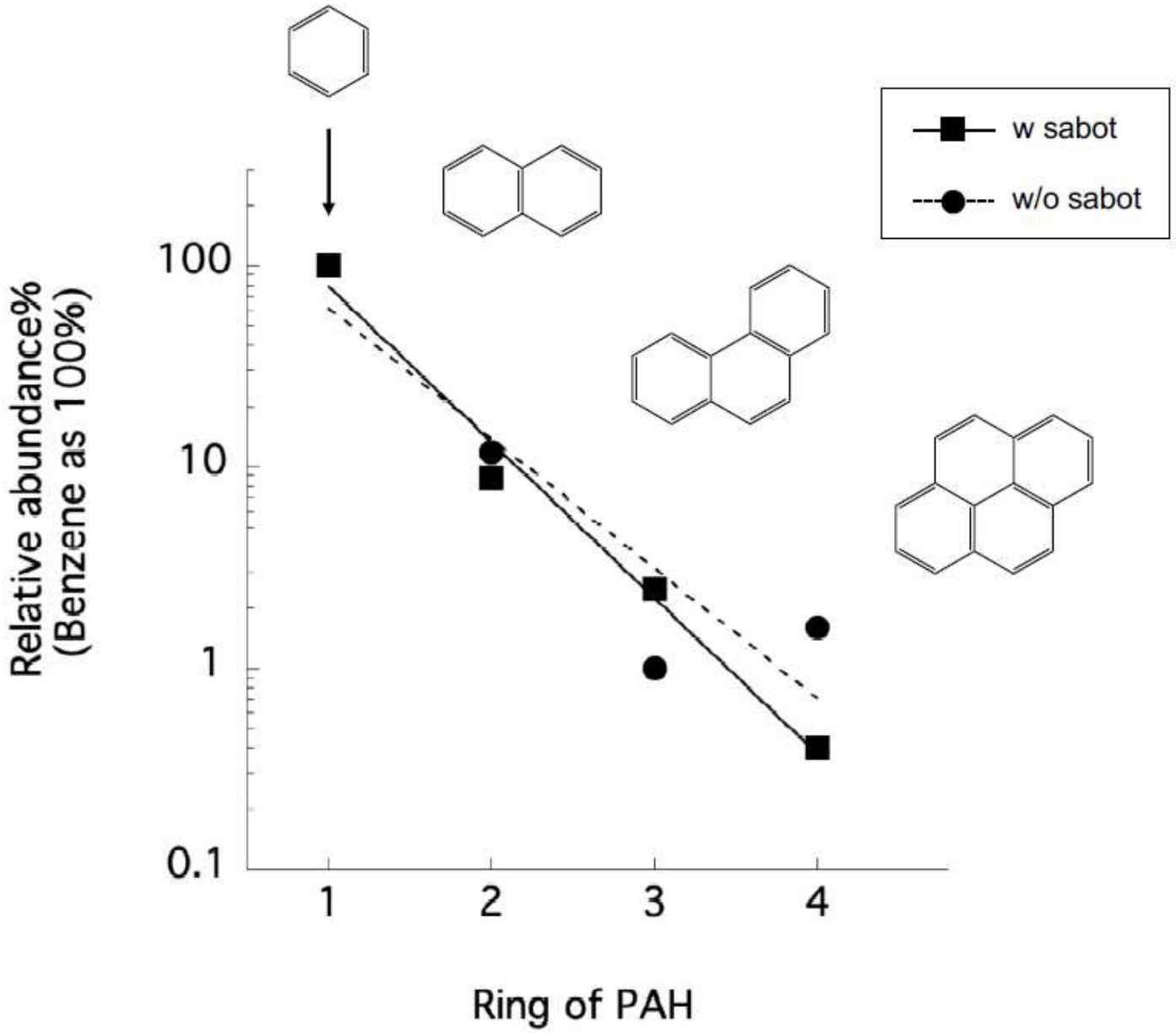

Figure 7

The relationship between the number of rings of the PAHs and their relative abundance normalized to benzene at 100. The abundance profiles were from benzene (monocyclic), naphthalene (bicyclic), phenanthrene (tricyclic), and pyrene (tetracyclic), where the concentrations of alkyl-PAHs were not included in the determination of each relative abundance. For further description of carbonaceous products, the detailed analysis of soluble organic matter using polar and apolar solvents will have to be performed by high resolution mass spectrometry with appropriate wet-chemical treatments (e.g., Orbitrap mass spectrometry by Oba et al., 2019; Isotope ratio mass spectrometry by Takano et al., 2015).

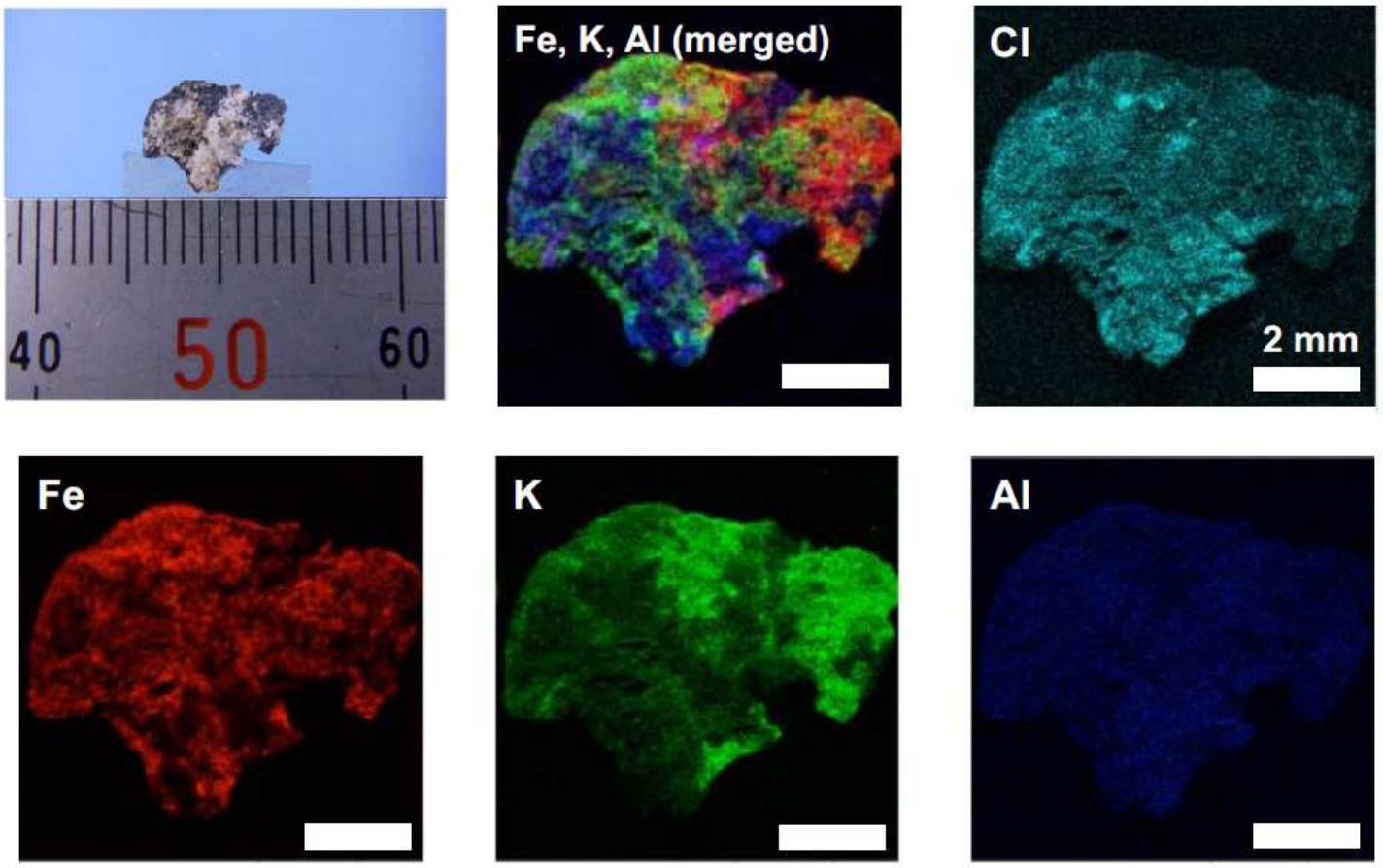

Figure 8

XRF surface imaging for representative elements (Fe, red; K, green; Al, blue; and Cl, light blue) for the carbonaceous products (the explosion experiment with the sabot). The white scale bar represents 2 mm.

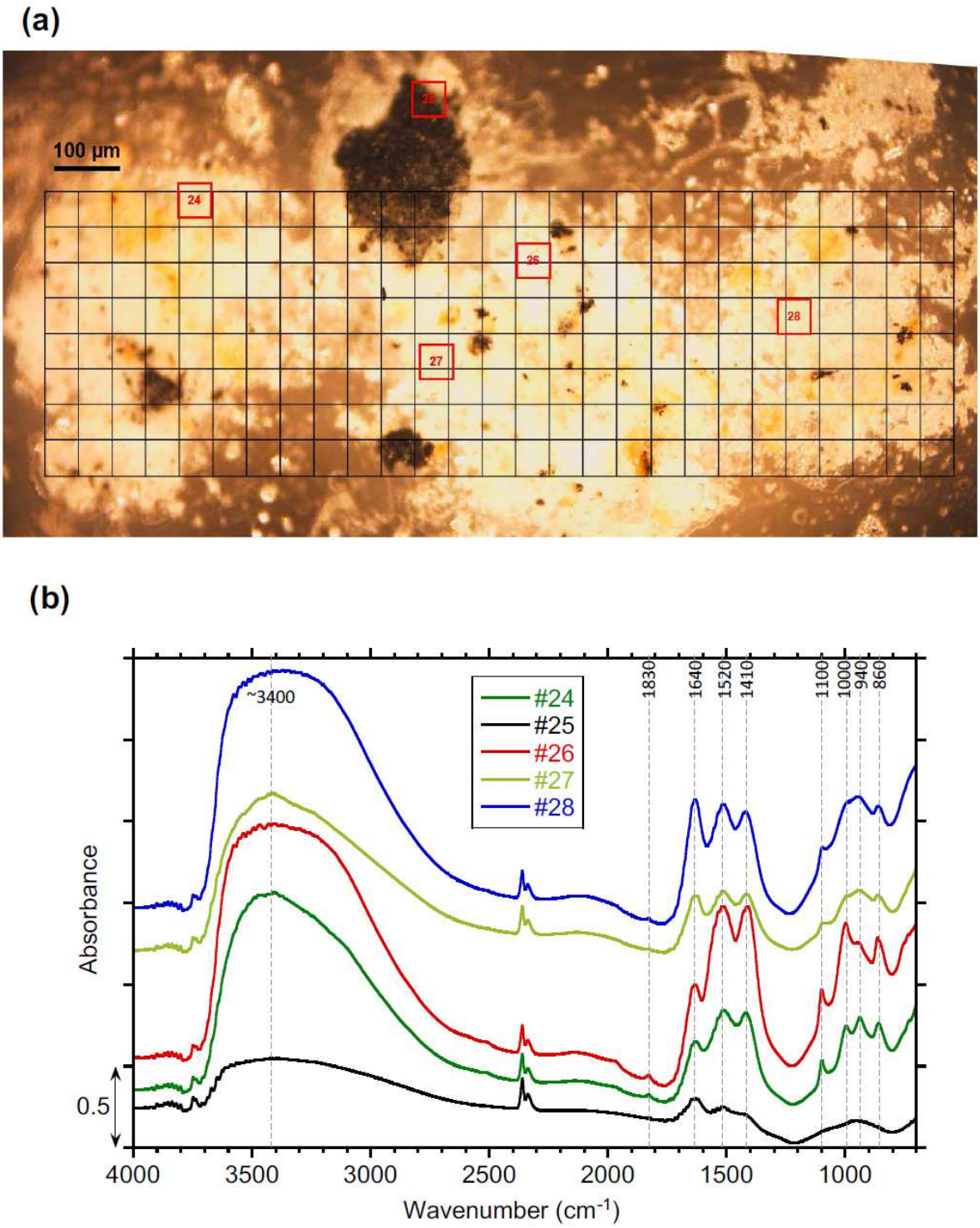

Figure 9

(a) Optical microscopy image of the carbonaceous sample from the quenched product. (b) IR spectral signatures obtained from the red squares (#24, 26-28 are from white materials and #25 is from black material). Possible peak assignments with references (Socrates, 2004) are shown in Table 1.

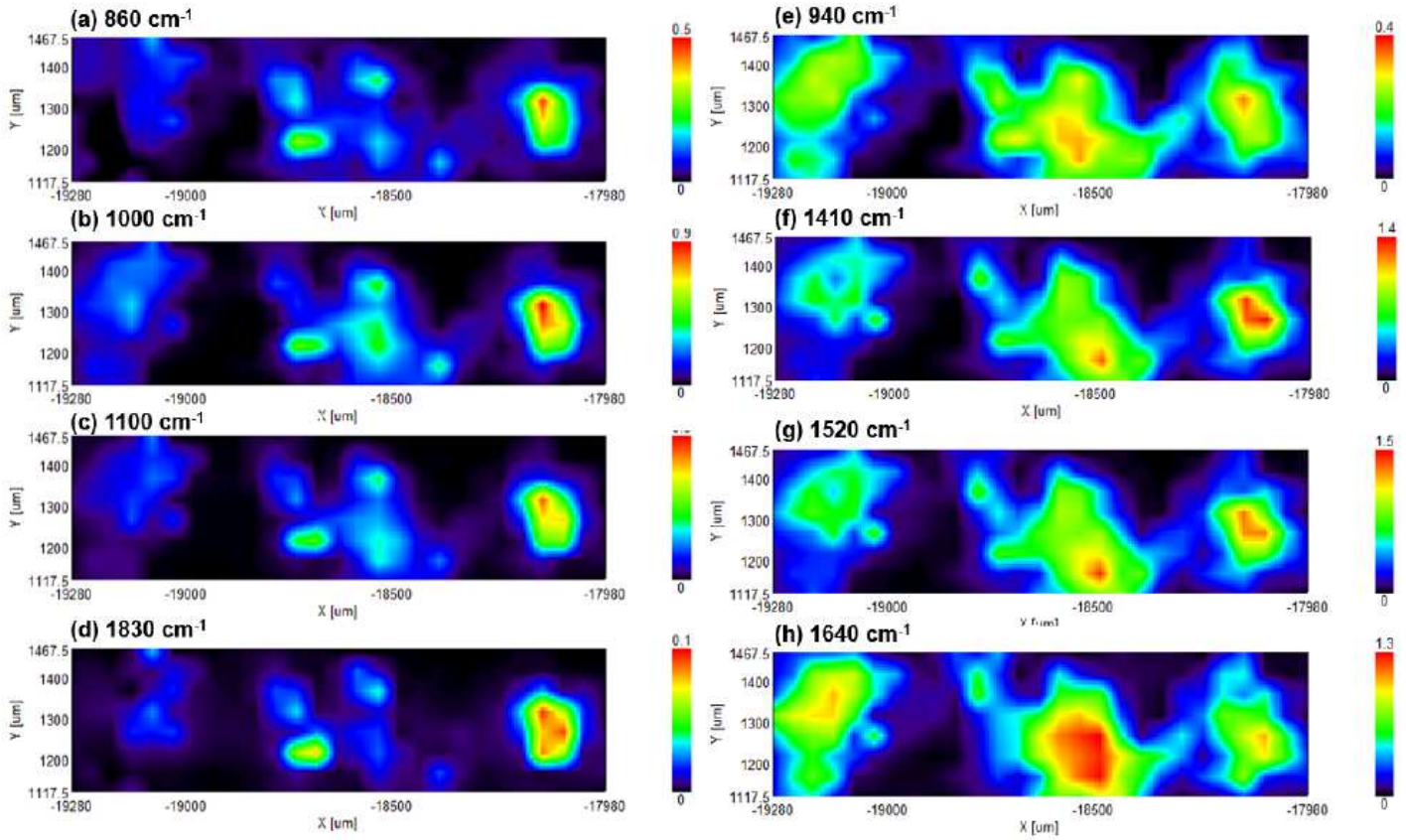

Figure 10

IR peak intensity maps at (a) 860 cm−1 with baseline between 780-1060 cm−1, (b) ~1000 cm−1 with baseline between 780-1060 cm−1, (c) 1100 cm−1 with baseline between 1060-1140 cm−1, (d) 1830 cm−1 with baseline between 1780-1860 cm−1, (e) 940 cm−1 with baseline between 780-1060 cm−1, (f) ~1410 cm−1 with baseline between 1250-1750 cm−1, (g) ~1520 cm−1 with baseline between 1250-1750 cm−1, and (h) ~1640 cm−1 with baseline between 1250-1750 cm−1. IR imaging on Figure 10 is corresponding to the region of interest in Figure 9.

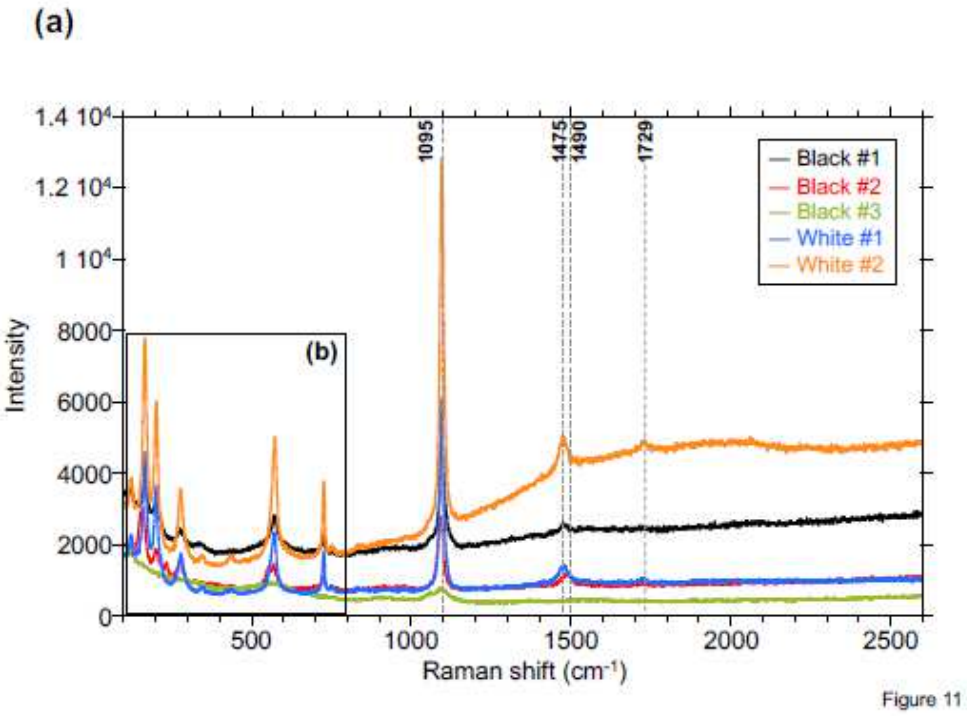

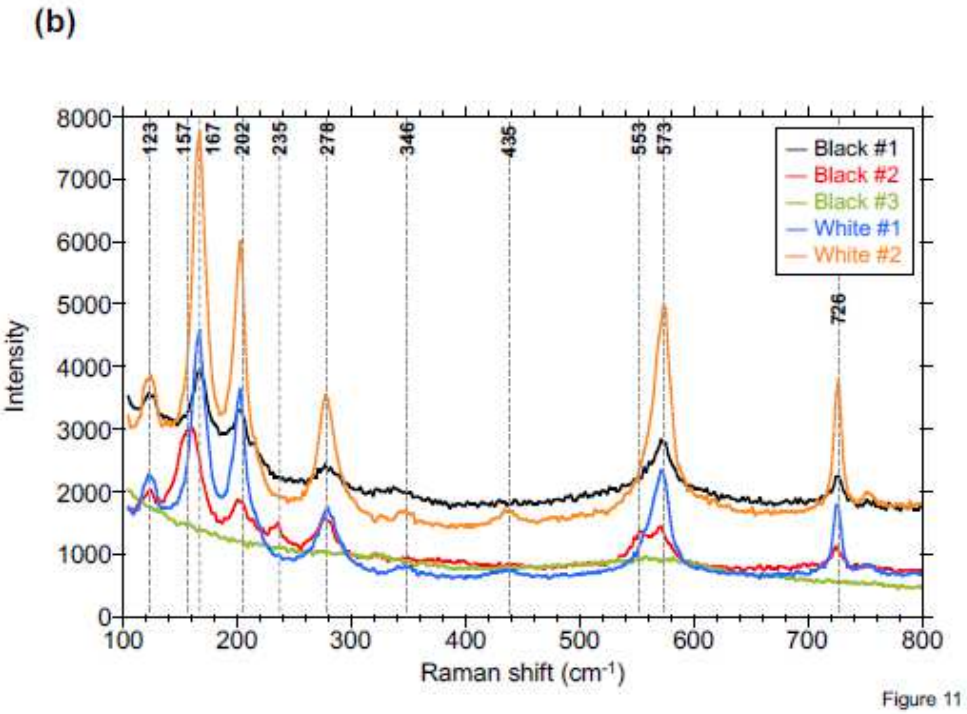

Figure 11

Raman spectra of the carbonaceous sample from the quenched product. “Black” indicates the spectra obtained from the black materials, and “white” indicates the spectra obtained from the white materials.

Supplementary Files

This is a list of supplementary files associated with this preprint. Click to download.

- 04GraphicalabstractEPS.pdf
- 03SIScriptEPSver200609revised.pdf